Impact of dewatering on pyrolysis oil upgrading: A comparative study of properties and hydrodeoxygenation

Downloaded from: https://research.chalmers.se, 2026-04-14 15:35 UTC

Citation for the original published paper (version of record):
Nejadmoghadam, E., Öhrman, O., Creaser, D. et al (2026). Impact of dewatering on pyrolysis oil upgrading: A comparative study of properties and hydrodeoxygenation. Chemical Engineering Journal, 533.
http://dx.doi.org/10.1016/j.cej.2026.174193

N.B. When citing this work, cite the original published paper.

research.chalmers.se offers the possibility of retrieving research publications produced at Chalmers University of Technology. It covers all kind of research output: articles, dissertations, conference papers, reports etc. since 2004. research.chalmers.se is administrated and maintained by Chalmers Library

(article starts on next page)

Chemical Engineering Journal 533 (2026) 174193

Contents lists available at ScienceDirect

Chemical Engineering Journal

journal homepage: www.elsevier.com/locate/cej

Impact of dewatering on pyrolysis oil upgrading: A comparative study of properties and hydrodeoxygenation

Elham Nejadmoghadam [a], Olov Öhrman [b], Derek Creaser [a], Louise Olsson [a,*]

[a] Chemical Engineering Division, Competence Centre for Catalysis, Chalmers University of Technology, Gothenburg, 41296, Sweden
[b] VAROPreem, Gothenburg, SE-418 23, Sweden

ARTICLE INFO

Keywords:
Pyrolysis oil
Upgrading
HDO
Dewatering
Sulfided NiMo/Al_2O_3 catalyst

ABSTRACT

Pyrolysis oil derived from residual biomass waste, such as sawdust, holds significant potential as a feedstock for biofuel production. However, due to its inherent properties, it cannot be directly processed in conventional hydrotreating reactors and requires pretreatment. The primary goals of upgrading pyrolysis oil via hydrotreatment are to reduce its oxygen content and facilitate the efficient separation of water. Dewatering pretreatment through azeotropic distillation with mesityl oxide offers a straightforward approach for partial upgrading, making it an attractive method for enhancing pyrolysis oil quality. In this study, pyrolysis oil underwent dewatering using this technique. The stability of the dewatered oil was evaluated through accelerated aging at 80 °C for 2 h and compared with untreated pyrolysis oil. The results indicated that the dewatered pyrolysis oil exhibited greater stability than the untreated sample under the aging treatment. The dewatered oil was subsequently upgraded by hydrodeoxygenation (HDO) using a NiMoS/Al_2O_3 catalyst to assess the impact of dewatering on the HDO process. Compared to untreated pyrolysis oil, the dewatered oil — characterized by reduced concentrations of acidic and carbonyl-containing compounds and reduced water content — yielded a higher proportion of deoxygenated products. This improvement was accompanied by increased water formation in a separated phase after reaction, attributed to HDO and condensation reactions, as well as a moderate increase in char formation. Notably, when water was reintroduced into the dewatered oil, catalyst inhibition effects reappeared, indicating that it is primarily the presence of water — rather than changes in the organic composition of the oil — that plays the dominant role in suppressing HDO performance.

1. Introduction

Harnessing biomass resources plays a vital role in mitigating environmental damage, enhancing economic stability amid fluctuating fossil fuel prices, and ensuring a sustainable future [1–4]. Biomass energy stands as one of the world's most significant renewable energy sources, contributing 77.4% to the global renewable energy supply and 10.4% to the total primary energy supply. Therefore, the efficient and sustainable utilization of biomass resources, particularly in the form of advanced biofuels, is essential for minimizing the environmental impacts associated with energy production [5].

The growing interest in biomass-based fuels and chemical compounds has driven research into conversion and upgrading pathways, which are key to commercializing these technologies [6]. In Sweden, around 16 TWh of low-cost biomass feedstocks including forest residues, sawdust, bark, and chips, are produced annually [7]. These materials hold significant potential as feedstocks for biofuel production, although they cannot be directly processed in conventional refinery hydrotreating reactors [8]. Fast pyrolysis, a relatively mature thermochemical technology, offers a promising solution by enabling the valorization of biomass [2,9,10]. This process has already been commercialized for producing renewable heating fuels and is also being explored for conventional fuel applications [10].

Bio-oils from fast pyrolysis offer several advantages over raw solid biomass, such as easier transportation, storage, and higher energy density [2,11]. With appropriate upgrading, these bio-oils have significant potential for widespread use. Fast pyrolysis oil has a brownish color with a smoky odor, and is a complex substance with a high oxygen content (28–40 wt%), similar to that of the raw biomass used in the pyrolysis process [12–14]. It also contains water, which is primarily produced from the dehydration of depolymerized carbohydrate products [9,12]. This composition contributes to the oil's high acidity,

* Corresponding author.
E-mail address: louise.olsson@chalmers.se (L. Olsson).

https://doi.org/10.1016/j.cej.2026.174193
Received 29 November 2025; Received in revised form 10 February 2026; Accepted 13 February 2026
Available online 3 March 2026
1385-8947/© 2026 The Authors. Published by Elsevier B.V. This is an open access article under the CC BY license (http://creativecommons.org/licenses/by/4.0/).

viscosity, relatively low heating value, and chemical instability due to the presence of numerous reactive species [2,15–18]. The oil is typically made up of various components, including water-insoluble high molecular weight compounds (15–23 wt%), organic molecules (20–30 wt %), water (19–30 wt%), and water-soluble substances (28–36 wt%) [12,19,20]. These characteristics make pyrolysis bio-oil unsuitable for direct use as a drop-in fuel without further processing [21]. Therefore, to produce a fuel-grade hydrocarbon from pyrolysis bio-oil and/or to be able to process fast pyrolysis bio-oil in conventional hydrotreating reactors, the removal of oxygen is essential, though this process can be costly [22]. Oxygen can be removed as water by reaction with hydrogen or as CO_2 and CO, which can reduce the final product yield [8,23]. The process of upgrading pyrolysis bio-oil to hydrocarbon fuel using hydrogen and a catalyst is known as catalytic hydrotreatment/hydrodeoxygenation upgrading [17,23]. However, this hydrogenation method suffers from catalyst deactivation issues caused by poisoning and fouling from reactive compounds such as carbonyl-derived polymers in the bio-oils and thereby their need for periodic regeneration [11,18,24,25]. Besides developing deactivation-resistant catalysts, pretreating pyrolysis bio-oil has been proposed as a means to achieve a stable subsequent hydrodeoxygenation (HDO) process [26,27]. A promising approach being explored is the stabilization of fast pyrolysis bio-oil, which involves removing or converting its reactive molecules. This process can enhance the bio-oil's properties and stability, thereby supporting hydrogenation and extending catalyst life, ultimately leading to a more effective upgrading into hydrocarbon biofuels [24,28]. Numerous approaches and methodologies are being investigated to stabilize and partially upgrade bio-oil [6,8,21,22,24,29–38]. These methods include mild catalytic hydrotreating to stabilize fast pyrolysis bio-oil [21,22,29–32,39–41], emulsification with surfactants and low molecular weight alcohols [39–41], the use of supercritical fluids with various organic solvents (ethanol, butanol, methanol, and acetone, etc.) [6,33,34], employing adsorbents to remove reactive carbonyl groups [24,35], co-processing in slurry reactors with hydrocracking catalysts and hydrogen [34,37,38], esterification and dewatering [8,36], and ultrasonic-assisted catalytic transfer hydrogenation [6].

Upgrading pyrolysis bio-oil mainly focuses on dewatering and deoxygenation [6]. It is commonly accepted that reducing the water content in pyrolysis oil can mitigate problems such as low heating value, chemical instability, corrosiveness and indeed modify its critical properties [11,42]. Numerous studies have been dedicated to dewatering pyrolysis oil derived from forest-based biomass, due to its low cost and ease of processing. The goal has been to enhance the quality and stability of the oil, making it more viable for further upgrading [8,10,11,25,36,43–45]. For example, Vitasari et al. [43] investigated the effect of water extraction on two pyrolysis oils derived from forest residue and pine. They found that this technique effectively recovered 80-90% of polar compounds and significantly reduced the complexity of the pyrolysis oil. The physical properties of dewatered oil obtained from pine wood-based pyrolysis oil using reduced pressure distillation, were assessed by Brodin et al. [10]. Their findings indicated that the oil quality was enhanced through a substantial decrease in water content and a partial reduction in acidity, as measured by the acid number. Other benefits of this treatment were an increase in energy content, a significant reduction in the corrosion rate, and a lower requirement for the co-solvent (n-butanol) needed to produce a homogenous and storage-stable multicomponent blend of dewatered oil and biodiesel. More recently, Khan et al. [11] compared two dewatering techniques—water extraction and reduced pressure distillation —for improving the properties of wood-derived pyrolysis oil. They found that pyrolysis oil dewatered by distillation, with a 60% reduction in water content, offered substantial advantages over untreated pyrolysis oil, including reduced corrosivity, higher heating values, increased carbon content, better thermal and storage stabilities, and increased potential for emulsification. In contrast, pyrolysis oil treated with water extraction exhibited higher corrosivity and negatively affected the emulsification properties.

In other studies, esterification combined with water removal has been assessed to achieve the dual benefits of reducing both acidity and water content of forest-based pyrolysis oils [8,25,36,44,45]. Reactive and azeotropic distillation have been key technologies for water removal, effectively reducing the water content of the oils, to near zero levels [8]. A range of entrainer solvents, including alcohols (n-butanol, and 2-ethylhexyl alcohol) [44], petroleum ether [36], and mesityl oxide [8], have been employed in azeotropic distillation to achieve these results.

Previous studies have mainly focused on the physical properties of pyrolysis oil subjected to dewatering techniques, describing the water content, acidity, miscibility, corrosiveness, emulsification potential and their contribution to esterification processes. However, none have addressed the catalytic hydrodeoxygenation of dewatered pyrolysis oil as a crucial pre-upgrading step — an area that this study aims to explore. Rather than employing the widely recognized two-stage hydrodeoxygenation (HDO) process, which involves catalytic hydrotreatment/stabilization at mild conditions (170-300 °C), followed by deep HDO at elevated temperatures (300-400 °C) [22,46], this work investigates an alternative, potentially more economical approach. According to our previous studies [21,32] on stabilization of simulated pyrolysis oil at mild conditions using various catalysts like conventional $NiMoS/Al_2O_3$ and several noble metal catalysts (alumina supported Pd, Rh, and Pt), it was found that, while some reactive oxygenated groups like furans and sugars were stabilized, undesirable polymerization also took place, resulting in the formation of solid. Herein, the quality of pyrolysis oil was improved using a two-stage upgrading strategy: initial dewatering treatment followed by catalytic HDO of the treated oil at high temperatures. This approach aims to partially upgrade the pyrolysis oil prior to catalyst exposure, thereby potentially mitigating catalyst deactivation and the need for subsequent regeneration. To our knowledge, this is the first effort to elucidate the impact of dewatering on subsequent hydrodeoxygenation and hydrogenation reactions during upgrading, as well as its potential influence on unwanted polymerization reactions that may lead to char formation. Accordingly, sawdust-derived pyrolysis oil, both untreated and dewatered, was upgraded under identical reaction conditions through catalytic hydrodeoxygenation using a conventional sulfided $NiMo/Al_2O_3$ catalyst in a batch reactor system. The resulting products were assessed using GCxGC/MS/FID, Karl Fischer titration, elemental analysis, ^{1}H NMR and 2D-HSQC NMR analyses. In addition, the general physicochemical properties of the feedstocks (pyrolysis oil and dewatered pyrolysis oil) were investigated, including water content, total acid number (TAN), elemental composition, carbonyl content, hydroxyl group quantification, and higher heating value (HHV).

2. Experimental

2.1. Catalyst synthesis and characterization

Catalyst synthesis and characterization were performed using standard procedures commonly reported in the literature [47–49]. A supported catalyst containing Ni and Mo was prepared by a conventional incipient wetness co-impregnation process using γ-Al_2O_3 (Puralox SCCA 150/200, Sasol). The ϒ-alumina support was first calcined at 550 °C for 8 h. Aqueous solutions of $Ni(NO_3)_2.6H_2O$ (Sigma-Aldrich) and $(NH_4)6Mo_7O_{24}.4H_2O$ (Sigma-Aldrich) were used as the precursors for the metals. The aqueous solution containing Ni and Mo was added dropwise to the support. The impregnated catalyst was dried in two steps: first at 60 °C for 12 h, then at 110 °C for another 12 h. This was followed by calcination at 550 °C for 12 h with a heating rate of 2 °C min^{-1} from room temperature.

The elemental composition of the catalyst was determined by Inductively coupled plasma sector field mass spectrometry (ICP-SFMS) performed by ALS Scandinavia in Luleå, Sweden. The surface area and

pore volume were measured by nitrogen physisorption using a TriStar 3000 gas adsorption analyzer with the BET (Brunauer–Emmett–Teller) and BJH (Barrett-Joyner-Halenda) methods. Catalyst samples were degassed at 200 °C before collecting N_2-physisorption isotherms at −195.8 °C.

2.2. Dewatering of pyrolysis oil

The pyrolysis oil was sourced from a commercial plant producing fast pyrolysis bio-oil from sawdust using the BTG-BTL (the Netherlands) technology. The dewatered pyrolysis oil, provided by VAROPreem (Sweden), was produced by batch azeotropic distillation of this commercial sawdust-derived pyrolysis oil [50]. A small-scale rotary evaporator at 60 °C with reduced pressure (around 20 mbar) was used; conditions suitable for heat-sensitive materials. Mesityl oxide (Chemtronica, Sweden) served as the entrainer solvent, as it forms an azeotrope with water and organic acids, enriching these components in the distillate [25]. During the distillation process, water and light organics soluble in the water-mesityl oxide azeotrope were removed, resulting in a highly viscous oil compared to the original pyrolysis oil. This product shall be referred to as dewatered pyrolysis oil (DPO). To further reduce its residual mesityl oxide content, the DPO was subjected to an additional evaporation step.

2.3. Pyrolysis oil upgrading procedure

Two bio-oil samples including fast pyrolysis oil (PO), and dewatered pyrolysis oil (DPO) used as feedstocks for this research were obtained from VAROPreem and were derived from softwood sawdust of Nordic origin. The catalytic hydrotreatment experiments using a $NiMo/Al_2O_3$ catalyst were conducted in a 450 ml Parr autoclave reactor system equipped with an impeller stirrer. The process of obtaining dewatered pyrolysis oil and the subsequent upgrading by catalytic hydrodeoxygenation is shown in Fig. 1.

All catalytic hydrodeoxygenation experimental conditions tested in this study are displayed in Table 1. In the first three runs, PO1, PO2, and PO3, the reactor was charged with 5 g PO, 80 ml hexadecane (≥99%, Sigma-Aldrich) a non-polar solvent for a 4 h reaction at various temperatures of 300, 350, and 400 °C, respectively. The catalyst was pre-reduced using 10 bar of H_2 at 450 °C for 4 h prior to these hydrodeoxygenation experiments. To analyze the effect of dewatering on pyrolysis oil, the DPO sample underwent hydrotreatment at similar experimental conditions as mentioned above (5 g DPO, 1 g reduced catalyst, 80 ml hexadecane, at 300 °C). However, due to the oil being very viscous, the experiment could not be completed because of severe solid formation. Therefore, in the next experiment (DPO1), this issue was addressed by reducing the amount of DPO while maintaining the same feed/catalyst ratio as in the previous experiments (DPO1: 2 g DPO, 0.4 g catalyst, along with 80 ml hexadecane solvent) and in addition the H_2 pressure was increased from 25 to 30 bar at room temperature. The

Table 1
Catalytic hydrodeoxygenation experimental conditions.

No.	Feed (g)	$NiMo/Al_2O_3$ (g)		Temperature (°C)
PO1	PO (5 g)	1	H_2 Reduced	300
PO2	PO (5 g)	1		350
PO3	PO (5 g)	1		400
DPO1	Dewatered PO (2 g)	0.4	DMDS	400
PO4	PO (2 g)	0.4	Sulfided	400
DPO2	Dewatered PO + water (2 g)	0.4		400

PO1, PO2, and PO3: HDO of pyrolysis oil at the temperatures of 300, 350, and 400 °C using reduced catalyst, DPO1: HDO of dewatered pyrolysis oil (2 g) at 400 °C using sulfided catalyst, PO4: HDO of pyrolysis oil (2 g) at 400 °C using sulfided catalyst, DPO2: HDO of (DPO + water: 2 g) at 400 °C using sulfided catalyst.

$NiMo/Al_2O_3$ catalyst was also pre-sulfided for this experiment using 200 µl dimethyl disulfide (DMDS, ≥ 99%, Sigma-Aldrich) at 340 °C and 20 bar hydrogen for 4 h, to improve its HDO activity [51]. Prior to the reaction, 100 µl DMDS was also added to the feed mixture, to maintain the catalyst in its sulfide state. The sawdust-derived pyrolysis oil used in this study contained a significant amount of water (22.6 wt%), comparable to the 22 wt% water content reported in the literature for wood sawdust pyrolysis oil [52]. To isolate and evaluate the specific effect of this inherent water content on the hydrotreatment process, 0.4 g of Milli-Q water was intentionally reintroduced to the dewatered pyrolysis oil (DPO) sample. This adjustment restored the water content to its original level, yielding a final sample containing 22.6 wt% water in a total of 2 g of oil. This mixture was then subjected to hydrotreatment under the same experimental conditions (DPO2) described previously (2 g feed, 0.4 sulfided catalyst, and 4 h reaction period, Table 1).

For comparison, the untreated pyrolysis oil as well as the rehydrated DPO sample underwent the HDO upgrading process under the same reaction conditions using 0.4 g sulfided catalyst (PO4, and DPO2). In all experiments, before starting the reaction, the reactor was purged three times with N_2 (8 bar) followed by further purging three times with H_2 (30 bar) prior to a leak test before being pressurized with H_2 to 30 bar at 25 °C. Then the reaction mixture was heated to the reaction temperature while stirring at 1000 rpm throughout the heating and constant temperature reaction period. After the 4 h constant temperature reaction period, the stirring and heating were stopped and the reactor was cooled down to 25 °C in a water bath. The reactor was finally purged with N_2 prior to collecting the upgraded oil products, catalysts, and residual solids. The vessel containing the upgraded oil was weighed and compared with the weight of the feed solution and the vessel's weight for mass balance determination.

$$Mass\ balance\ (\%) = \frac{\sum (\text{Mass of product(s)})}{\text{Mass of pyrolysis/dewatered } oil} \times 100 \quad (1)$$

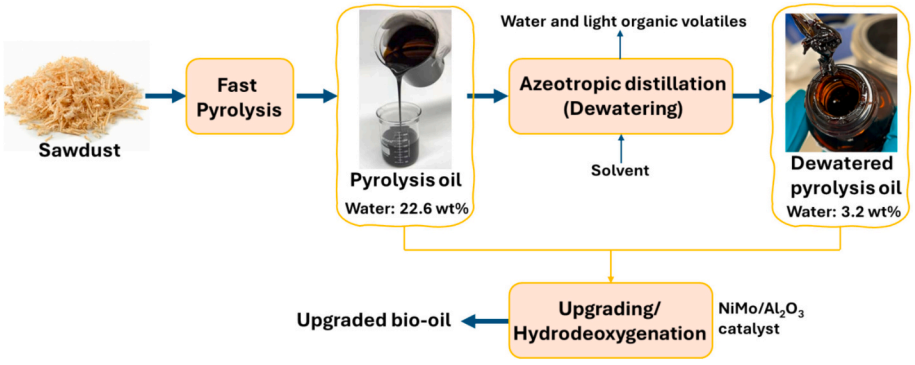

Fig. 1. Overview of the process for producing and upgrading dewatered pyrolysis oil.

The residual difference from this comparison ranged from 2.2 to 3.9 wt%, suggesting some material losses and/or gas formation occurred. The solid and liquid fractions were separated using vacuum filtration and a glass filter. The organic phase, rich in hexadecane, was collected and the reactor was washed with acetone to recover any residual organics and solvent. After filtration, the resulting acetone-rich mixture was termed the aqueous phase. The remaining solid was dried at 90 °C overnight, weighed, and labeled as the 'total solid product' excluding the catalyst. Following the protocol from our previous studies [21,32], the solid products obtained from the PO1, PO2, and PO3 experiments were subsequently washed with dimethyl sulfoxide (DMSO, ≥99%, VWR) to extract soluble components from a char-like material (insoluble solids). However, this procedure was not continued in the other experiments (DPO1, PO4, DPO2) because the solids obtained at high temperature were predominantly composed of DMSO insoluble fractions. The water content in both the aqueous and organic phases was measured using volumetric Karl-Fisher titration. Both phases were then analyzed using GC × GC–MS-FID analysis for chemical characterization. Additionally, two-dimensional heteronuclear single-quantum coherence NMR (2D-HSQC-NMR) and ^{1}H NMR were used to analyze the two feedstocks, as well as the upgraded oils obtained from hydrotreatment of PO and DPO (PO4, and DPO1), respectively.

In this study, the stability of these two oils, PO and DPO, was also assessed using an accelerated aging process using 2 g of oil with 80 ml of hexadecane solvent in a batch reactor at 80 °C for 2 h, under a N_2 atmosphere, following the method outlined in our previous work [32]. The aged oils were referred to as 'Aged PO' and 'Aged DPO'. The procedure for collecting the aged oils and their characterization is illustrated in Fig. S2 in the Supplementary Information (SI).

2.4. Feedstocks and product characterization

2.4.1. Two-dimensional gas chromatography (GC × GC–MS-FID)

Two-dimensional gas chromatography with flame ionization detection (GC×GC-FID) and mass spectrometry (GC×GC–MS) analyses were performed using an Agilent 7890B-5977 A system on pyrolysis oils, aged oils, and upgraded oils. Two columns, a mid-polar column (VF-1701MS, 30 m × 250 μm × 0.25 μm) and a non-polar DB-5MS (1.2 m × 150 μm × 0.15 μm) were used for the separation. The oven temperature was initially set to 40 °C for 4 min, then gradually increased to 280 °C at a rate of 3 °C per minute. Thermal modulation was maintained at 5 s for all samples. The flame ionization detector was held at 250 °C. Helium gas was used as a carrier with a flow rate of 0.8 ml/min with a split ratio of 5. The resulting 2D chromatograms (MS-FID) were thoroughly analyzed using GC Image software. According to various reports on the analysis of complex bio-oil mixtures [53,54], GC methods face limitations due to i) sample volatility, as nonvolatile, high-molecular-weight bio-oil compounds are typically undetectable, ii) the unavailability of analytical standards for many bio-oil compounds, and ii) the unavailability of the MS spectra for certain bio-oil compounds in MS libraries. In this study, the GC analysis was performed based on the peak volumes of identified compounds to represent a part of the chemical composition of the pyrolysis oil feedstocks and upgraded oil samples. The analysis categorized the oil samples into identified and unidentified compounds, with the latter including heavy oligomers and compounds unidentifiable by mass spectrometry. This approach aligns with methodologies in other studies that similarly focus on a subset of the oil's composition [54,55]. Compounds were identified by comparison of their mass spectra with the standard spectra in the National Institute of Standards and Technology (NIST) library and were grouped into various chemical classes which are explained more in Section 3.1.

2.4.2. TAN number

To evaluate the acidity of pyrolysis oil and dewatered oil, the Total Acid Number (TAN)—which indicates the concentration of acidic compounds in bio-oil [56]—was measured using automatic titration. The procedure employed an Orion Star T910 titrator with a pH probe, following a modified ASTM D664 method developed by Agblevor et al. [57]. In this method, aqueous potassium hydroxide (45 wt% KOH) diluted to 0.1 M in Milli-Q water was used as a standard titrant, while acetone served as the titration solvent. A 0.1 g bio-oil sample was dissolved in 50 ml of acetone and titrated with KOH until the pH reached 11. The TAN, expressed in mg of KOH per gram of oil (mg KOH/g oil), was calculated based on the difference in the volume of KOH (in ml) added between the sample and a blank. The calculation also accounted for the KOH solution concentration (N_{KOH} in mmol/ml), the molecular weight of KOH (M_{KOH} in mg/mmol), and the sample weight (in g), as shown in Eq. 2. This procedure was conducted three times for both the blank and the bio-oil samples, with the average value being reported.

$$TAN = \frac{V_{KOH(sample-blank)} . N_{KOH} . M_{KOH}}{\text{sample weight}} \quad (2)$$

2.4.3. Carbonyl content

The carbonyl content in pyrolysis bio-oils was quantitively measured using a modified Zakas/Faix procedure that was developed by the National Renewable Energy Laboratory (NREL) group [58]. The titration methodology is as follows: solutions of hydroxylamine hydrochloride ($NH_2OH{\cdot}HCl$) and triethylamine (TEA) were prepared. The bio-oil sample was diluted in a suitable solvent, DMSO, followed by the sequential addition of $NH_2OH{\cdot}HCl$ and TEA solutions. This procedure was performed in triplicate for each sample, as well as for the blank samples (DMSO, TEA and $NH_2OH{\cdot}HCl$ solution). The mixture was placed into 5 ml Reacti-vials that are equipped with a conical magnetic stirrer and heated in a preheated dry block heater at 80 °C for 2 h with stirring. $NH_2OH{\cdot}HCl$ reacts with carbonyl groups, and TEA acts as a buffer to ensure the oximation reaction reaches completion. After the reaction, the solution was quantitatively transferred to a titration cup with ethanol and water and titrated against a standardized HCl solution (0.1 M) using an automatic potentiometric titrator. The equivalence point occurred around pH 3.5. The carbonyl content (wet basis) was calculated using eq. 3:

$$\text{Carbonyl content} = \frac{(a_0 - a)}{wt} \times N \ (\text{mmol/g}) \quad (3)$$

a, a_0 = volumes of 0.1 M HCl (ml) used for titration in bio-oil sample and the blank, respectively.

N = concentration of the HCl titrant (0.1 M HCl, mol L^{-1}).

wt = weight of oil sample (g).

2.4.4. P-NMR

The hydroxyl groups in pyrolysis bio-oils were characterized and quantified by 31-P nuclear magnetic resonance (P-NMR) analysis after a phosphitylation pre-treatment using 2-chloro-4,4,5,5-tetramethyl 1,3,2-dioxaphospholane (TMDP) according to the literature [59–61]. Various hydroxyl groups (mmol/g) were measured using N-hydroxy-5-norbornene-2,3-it dicarboximide (NHND) [32,61] as the internal standard (IS). Topspin software (Bruker) was used for baseline and phase adjustments as well as peak integration.

2.4.5. NMR

^{1}H and two dimensional (^{1}H – ^{13}C) heteronuclear single-quantum coherence (HSQC) NMR spectroscopy at 800 MHz were employed to characterize the two pyrolysis bio-oils and their corresponding hydrotreated products following upgrading. Samples were dissolved in deuterated chloroform ($CDCl_3$), which also served as the reference solvent for chemical shift calibration, following the method outlined in our previous study [21]. Data processing was done using MestRenova software.

2.4.6. Karl Fischer titration

For determination of the water content present in the two pyrolysis

bio-oil samples along with their corresponding aged products and upgraded oils, Karl Fischer titration (870 Titrino Plus, Metrohm) was conducted. Following calibration of the instrument with a water standard (Honeywell Fluka), a small oil sample was injected into the glass chamber containing Hydranal (Honeywell Fluka) and automatically titrated with Karl Fischer titrant composite 5 (Honeywell Fluka). This procedure was repeated in triplicates, and the average value was recorded.

2.4.7. GPC

The average molecular weight of the pyrolysis bio-oil and dewatered pyrolysis oil were measured by gel permeation chromatography (GPC) using two PolarGel-M columns (300 × 7.5 mm) and a pre-column (PolarGel-M, 50 × 7.5 mm) in a system with an ultraviolet light (UV) detector operating at 280 nm. The detailed methodology is given in our previous work [32]. In brief, prior to GPC analysis the samples were dissolved in the eluent — DMSO containing 10 mM LiBr — filtered through a 0.2 μm GHP syringe filter, and analyzed in duplicate. The column oven temperature was maintained at 50 °C, with a flow rate of 0.5 ml/min. The GPC system was calibrated using pullulan standards and data analysis was performed with Cirrus GPC Software version 3.2.

2.4.8. Elemental analysis

The elemental composition of the pyrolysis bio-oil samples and the spent catalysts containing deposited solid products was determined through elemental microanalysis (Devon, U.K.) using the Dumas combustion method for C, H, N, and S and the Unterzaucher pyrolysis method for O analysis. Due to the fine nature of the catalyst particles, separation of the solid deposits from the catalyst was not feasible. Each analysis was conducted twice, and the average value is reported. Reported H/C and O/C ratios are an average from two repeated measurements.

2.4.9. Higher heating value (HHV)

The HHV of oil samples was calculated based on the average of two measurements detecting the composition of the main elements, carbon (C), hydrogen (H), and oxygen (O), in wt%, using the Channiwala and Parikh formula (Eq. 4) for liquid fuels, that produces results in good correlation with calorimetric measurements of HHV [62].

$$HHV = C \times 0.3491 + H \times 1.1783 + S \times 0.1005 — O \times 0.1034 — N \times 0.0151 \; MJ \bullet kg \quad (4)$$

3. Results

3.1. Pyrolysis oil and dewatered pyrolysis oil properties

Table 2 presents a comparative analysis of various representative physicochemical properties of the pyrolysis oil, and dewatered oil, including the elemental composition, heating value, water content, and average molecular weights. An oxygen content of 43.7 wt% was obtained from elemental analysis of the pyrolysis oil including both oxygen in organics and as water. Since the pyrolysis oil contained 22.6 wt% H_2O, its oxygen content on a dry basis was 30.5 wt%, which is lower than the oxygen content of the dewatered pyrolysis oil — 32.9 wt% on a dry basis and 34.7 wt% when including water. The inclusion of mesityl oxide in the dewatering process of the pyrolysis oil can be a reason for the moderately increased oxygen content in the resulting dewatered oil sample. Consistent with previous research [11], a strong inverse correlation was observed between water content and the higher heating value of the pyrolysis oil. The distillation process improved the heating value by 32% through effective water removal (Table 2). However, it remains lower than that of crude oil. This treatment also resulted in a small molecular weight reduction. Additionally, the water removal treatment led to an increased carbon content while slightly decreasing hydrogen levels. This suggests the removal of more hydrogen-rich components occurred, leaving a residue with a lower H/C ratio. Consequently, the reduction in oxygen content and the increase in carbon content contributed to a higher HHV of the dewatered pyrolysis oil. Nevertheless, according to the recommendations of the NREL Thermochemical Group [9,63], which stipulate that the oxygen content must be reduced below 7 wt% for the oil to be deemed stabilized and suitable for coprocessing in a petroleum refinery, the dewatered oil with its current oxygen content of 34.7 wt% does not meet these stabilization criteria.

Carbonyl compounds, produced through thermal decomposition during the pyrolysis process [66], play a key role in changes to bio-oil properties during storage and upgrading [24,58,67], due to their high reactivity causing instability issues [24]. As a result, numerous studies focus on quantifying carbonyl content in bio-oils [22,24,53,58]. Another approach to characterizing pyrolysis oil involves measuring the TAN, which accounts for carboxylic acids as well as weaker acidic compounds such as phenolics [24,53]. In this study, both carbonyl content and TAN were measured to compare pyrolysis oil and dewatered oil, as displayed in Fig. 2. Bio-oils typically contain carbonyl groups ranging in concentration from 4 to 6 mmol/g [22]. Herein, after the dewatering process, the carbonyl content decreased from approximately 4 mmol/g to 2.2 mmol/g (Fig. 2b). This reduction indicates a lower concentration of water-soluble carbonyl compounds, contributing to an overall decrease in carbonyl content that could improve the bio-oil's stability and

Table 2
Relevant Properties of the bio-oils including pyrolysis oil and dewatered oil used in this study.

	Sawdust-based pyrolysis oil	Dewatered pyrolysis oil		Fossil [64]	
			Crude oil [65]	Vacuum gasoil	Diesel fuel
Elemental composition					
H (wt%)	7.3 ± 0.01	6.5 ± 0.02	12	–	–
C (wt%)	42.5 ± 0.02	57.2 ± 0.00	85	–	–
O (wt%)	43.7* ± 0.13	34.7* ± 0.03	3.6	–	–
S (wt%)	<0.1	<0.1	–	0.59-0.67	<0.001
N (wt%)	<0.05	<0.05	1.3	0.33-0.34	–
H/C ratio	2.1	1.36	1.69	1.6	1.85
O/C ratio	0.75	0.33	0.03	<0.01	–
HHV (MJ/Kg)	18.9* ± 0.02	24.0* ± 0.02	42.9	–	–
Water wt%	22.6 ± 0.32	3.2 ± 0.22	0.1	0.1	
Average M_w (g/mol)	1106	1040			
Aliphatic OH (mmol/g)	3.8	4.8			
Phenolic OH (mmol/g)	2.3	2.9			
Carboxylic OH (mmol/g)	0.5	0.7			

(O (wt%)*: wet basis for pyrolysis oil and dewatered oil)
(*HHV: Higher heating value obtained from Channiwala and Parikh formula [62])

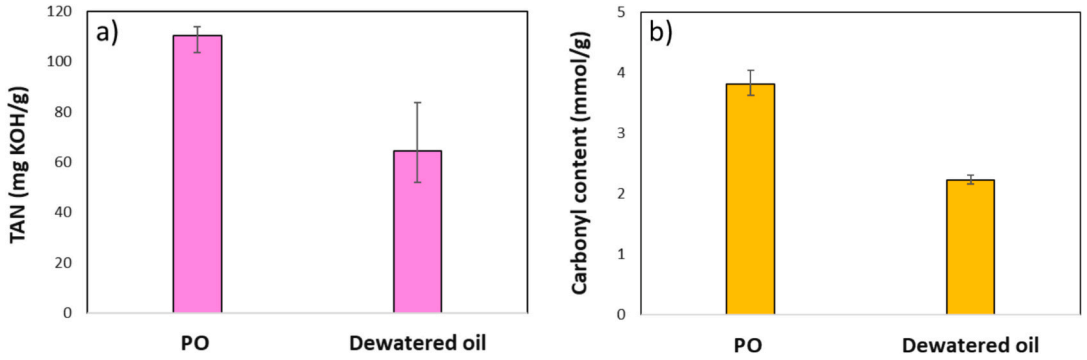

Fig. 2. Comparison of a) TAN (mg KOH/g), and b) carbonyl content (mmol/g) of pyrolysis oil (PO) and dewatered pyrolysis oil (DPO).

decrease its reactivity.

The acidity of pyrolysis bio-oils is primarily attributed to volatile acids (60-70%), with additional contributions from phenolics, fatty and resin acids, and hydroxy acids [56]. According to Fig. 2a, the total acid number of the dewatered oil decreased by 41% compared to the original PO, suggesting that volatile acids were likely removed during the dewatering process. This finding aligns with literature reports, indicating a significant reduction in TAN due to the removal of water soluble

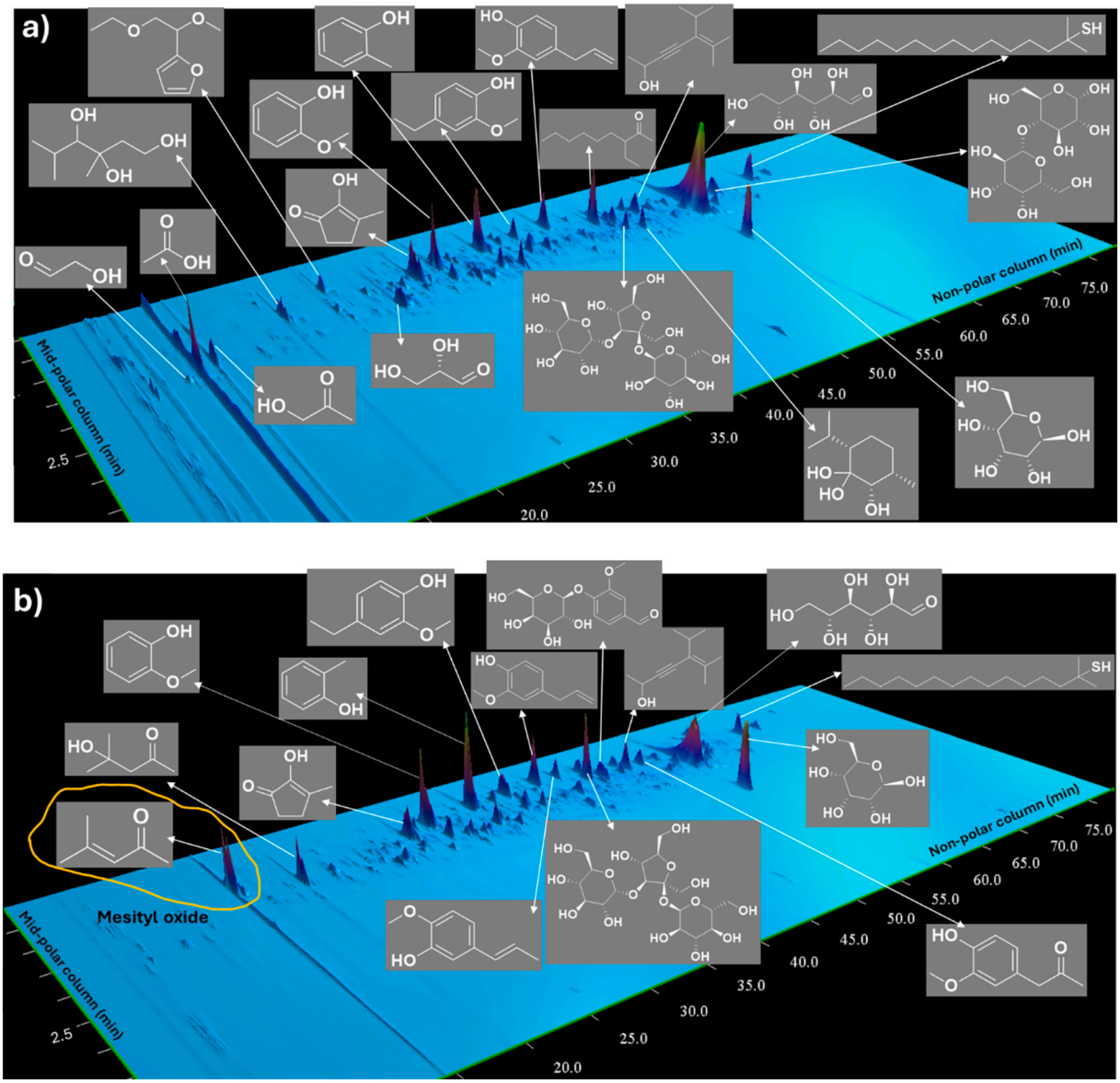

Fig. 3. 3D spectral plots of GCxGC chromatograms illustrating the chemical structures of the primary compounds identified in: a) pyrolysis oil, b) dewatered pyrolysis oil, and c), d) aged pyrolysis oil and aged dewatered pyrolysis oil, respectively.

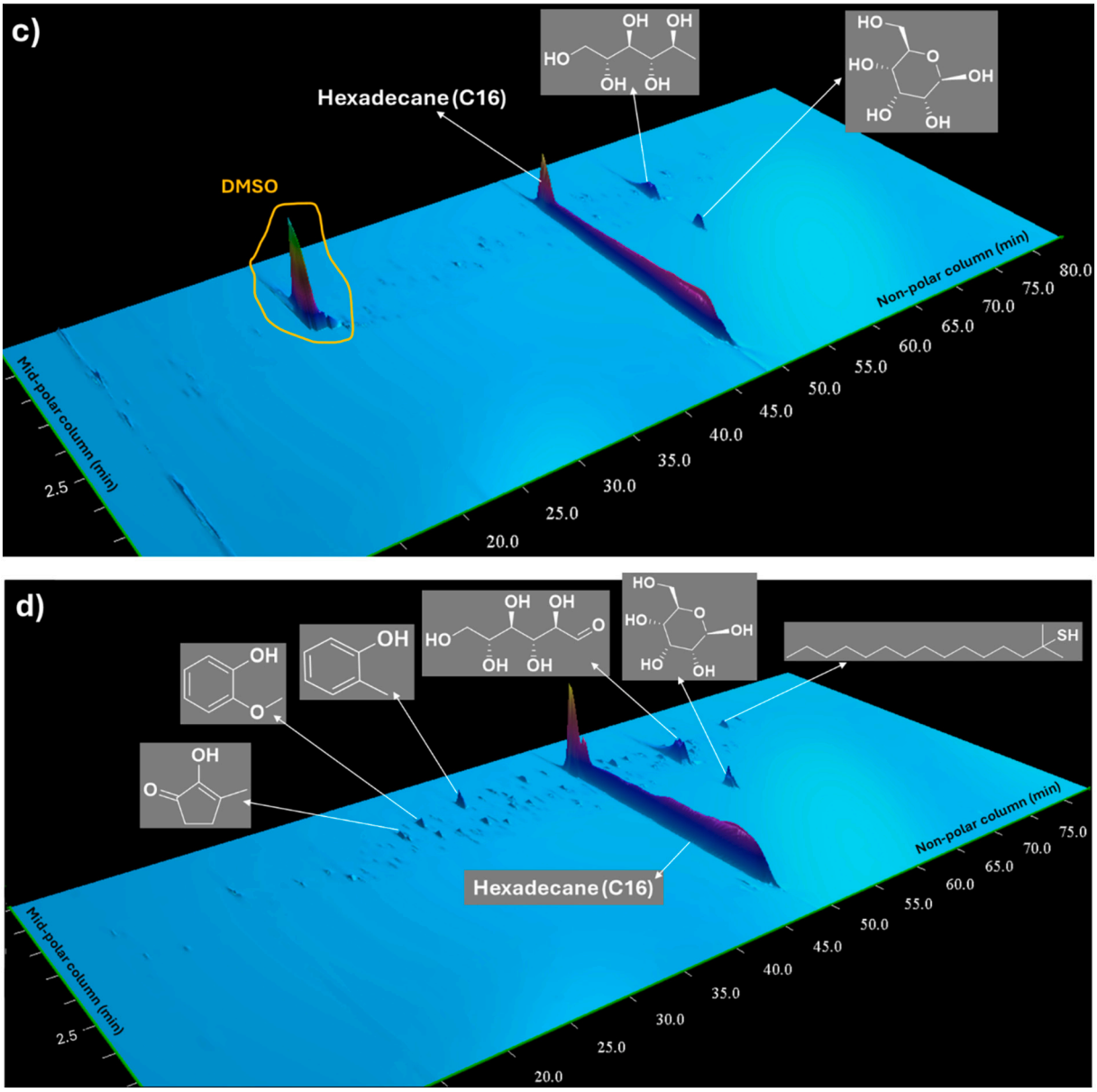

Fig. 3. (*continued*).

compounds from pyrolysis oil derived from forest biomass [36]. It is crucial to note that, when comparing TAN values of pyrolysis bio-oils from different sources or pyrolysis conditions, the specific acidic components must be considered, as standard TAN measurements may not be directly comparable [68]. Furthermore, the slight reduction in the average molecular weight of the dewatered oil compared to the original pyrolysis oil (Table 2) suggests that more than just light or volatile components were removed. If only those components had been extracted, an increase in the average molecular weight would be expected.

The molecular composition of the two bio-oil feedstocks — pyrolysis oil and dewatered pyrolysis oil — as well as their corresponding aged oils following accelerated aging, was determined using GCxGC–MS/FID, as shown in Figs. S1 and 3. The most abundant GC detectable low molecular weight compounds, corresponding to the most intense chromatographic peaks and their retention times, are listed in Table S1 and illustrated in Fig. 3. Compounds identified by GC with a low matching probability (below 10%) using the NIST library were categorized as 'unidentified' components, which accounted for approximately 27-30% of the GC/MS detectable compounds in the pyrolysis oil composition. Additionally, heavier oligomers beyond the detection range of GC are also present in the pyrolysis oil.

Hundreds of compounds belonging to various organic groups were identified and classified into chemical groups, such as acids, sugar derivatives (including aldehydes, ketones, furans and sugars), phenolics, esters/ethers, alcohols, hydrocarbons, and multiple oxygenates containing more than one functional group. The retention time distribution of these compound groups in pyrolysis oil and dewatered pyrolysis oil is shown in Figs. S1a and S1b, with the regions labeled 1-10.

Fig. 4 displays the overall peak volume percentages of the organic compound groups identified in each classification. In addition to these identifiable compounds, there are unresolved blobs in the GCxGC chromatograms that could not be identified using the NIST library. It should be noted that large oligomers fall outside the detection range of GCxGC and are therefore not represented. The results indicate that the original pyrolysis oil is mainly composed of sugars (26%), acids (10%), and multiple oxygenates (9%), highlighting its richness in oxygenated compounds (Fig. 4a). It also contains 8% phenolics, 6% aldehydes/ketones, and 7% esters/ethers, along with traces of alcohols, and

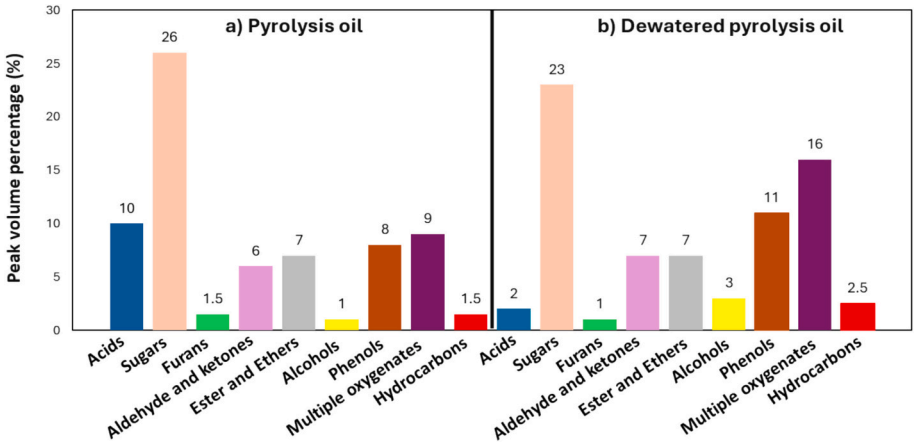

Fig. 4. Distribution of various organic compound groups present in original pyrolysis oil and dewatered pyrolysis oil.

hydrocarbons (1% and 1.5% respectively). From Fig. 4a, the dominant compounds include acetic acid, levoglucosan, cresol, eugenol, 3-ethyl-2-nonanone, 2-methoxyphenol, cyclotene, etc. This observation is in line with the composition of pyrolysis oil reported in previous studies, which report that pyrolysis oil mainly consists of phenols, acids, and sugars [53,69].

However, following the water removal treatment, notable changes in oil composition were observed (Figs. S1b, 3b, and 4b). Most prominently, the acetic acid peak — marked as region 2 at a retention time of 9 min × 3.6 min in Fig. S1b — nearly disappeared, with its peak volume percentage dropping from 10% in the original pyrolysis oil to just 2% in the dewatered oil (Fig. 4). Additionally, the peak volume percentages of sugars (e.g. levoglucosan), and furans also decreased (Figs. 3 and 4b), suggesting that these highly reactive compounds were extracted along with the water.

Due to their high polarity and water solubility, compounds such as acetic acid and to some extent, levoglucosan, were preferentially collected in the aqueous phase during the dewatering process, facilitating their removal from the pyrolysis oil. These findings are consistent with the study by Vitasari et al. on water extraction from pyrolysis oil [43]. In addition to water solubility, the solubility of compounds in mesityl oxide should also be considered when evaluating dewatering efficiency. During the azeotropic distillation process, the content of phenolics, and multiple oxygenated compounds increased to 11% and 16% respectively, while the oil remained rich in sugars (23%). The selective removal of certain organic compounds — those more soluble in water and/or mesityl oxide — led to a slight decrease in the average molecular weight of the treated oil, as shown in Table 2. It is also important to note that while some oxygenates were removed because of the azeotropic distillation, mesityl oxide was introduced into the oil. As indicated in Fig. 4b, mesityl oxide contributed to 11% of the total peak volume within the ketone/aldehyde group of the dewatered pyrolysis oil.

3.2. Aging of pyrolysis oil and dewatered pyrolysis oil

To track the aging characteristics of pyrolysis oil and dewatered pyrolysis oil, both were subjected to accelerated aging at 80 °C for 2 h (Fig. S2). Their chemical composition, water content and molecular weight were subsequently analyzed. During aging, no solids formed in the pyrolysis oil; however most light GC-detectable compounds — including highly reactive carbonyls such as acids, aldehyde/ketones, as well as sugars, and phenols (Fig. 4a) — were converted into GC-undetectable heavy oligomers. This transformation resulted in the disappearance of many chromatographic peaks compared to the fresh PO, with only a few compounds, such as sugars like levoglucosan and D-allose, remaining detectable (Fig. 3c). Similarly, in our previous study on the aging of simulated pyrolysis oil containing representative organic compounds (e.g., acetic acid, levoglucosan, benzaldehyde, hydroxyacetone, HMF, and guaiacol) aging led to their conversion into heavier products, leaving no light compounds detectable by GC [32]. However, a known artifact from DMSO contamination appeared as a prominent peak in the GCxGC analysis, as highlighted in Fig. 3c. Another notable finding was the increase in water content in the aged PO — from 22.6% to 25.3 wt% — suggesting the formation of extra water during aging. This observation aligns with literature indicating that water content typically rises during pyrolysis oil aging [70,71]. Various reactions, including dehydration, self-condensation, esterification, aldol condensation, and interactions between phenols, and aldehydes likely contributed to the transformation of reactive compounds during the aging process [70,72–74].

However, during the aging of dewatered oil (DPO), which has a distinct chemical profile characterized by a much lower acid content, reduced initial water content (3.2 wt%), and lower carbonyl levels, a slight drop in water content to 2.6 wt% was observed. This reduction may be attributed to polymerization or hydration reactions, which consume water during accelerated aging, aligning with the observations of Sui et al. [75] on aging of pyrolysis oil derived from cotton stalk. However, given the high viscosity of the dewatered oil, the small difference between 3.2 and 2.6 wt% could also be due to sample variability. No solid formation occurred, and the average molecular weight only increased slightly to 1051 g/mol. It is known that the presence of organic acids in pyrolysis oil can accelerate aging [72], acting as both reactants and catalysts [73]. Therefore, the lower concentration of acids in the DPO, might suppress reactions such as esterification, acetalization, dimerization, etc. [72]. Furthermore, the lower sugar content in DPO may contribute to improved bio-oil stability, as previously reported [76]. According to the GC analysis results, certain compounds — including sugars (levoglucosan, D-allose), phenols (2-methoxyphenol, cresol), and furanic compounds (cyclotene) — remained detectable after aging (Fig. 3d), although there were overall significant changes in the GC spectra due to the aging.

In conclusion, the dewatered pyrolysis oil, due to its distinct composition, underwent less degradation during aging compared to the original pyrolysis oil. This might be attributed to its lower concentration of acid and carbonyl compounds, which limit the extent of aging-related reactions.

3.3. Pyrolysis oils upgrading

Catalytic hydrotreatment was carried out on two feedstocks, pyrolysis oil and dewatered pyrolysis oil, using the prepared $NiMo/Al_2O_3$ catalyst at various reaction conditions for 4 h. The catalyst's active metal content and textural properties (characterized by BET in duplicate) are

summarized in Table 3. All experiments yielded three distinct phases after reaction: solid, liquid(s), and gaseous products produced from the HDO reactions.

In the first three experiments (PO1-PO3) on pyrolysis oil using the H_2 reduced $NiMo/Al_2O_3$ catalyst (1 g), the solid yield decreased significantly — by 74% — by increasing the temperature from 300 to 400 °C (Fig. S3). This result suggests that higher temperatures are critical for suppressing the formation of undesired solid products and promoting favorable HDO reactions [21].

Accordingly, the subsequent experiments (DPO1, and PO4) were conducted at 400 °C, maintaining the same feed/catalyst ratio of 5, but using the sulfided catalyst (0.4 g) for HDO of both dewatered oil and pyrolysis oil (each 2 g). These experiments were carried out in duplicate, and the corresponding mean results with standard deviations are presented in Table S2. Fig. 5 illustrates that catalytic HDO of dewatered oil (DPO1) resulted in a higher solid yield (7.3 wt%) compared to the pyrolysis oil (PO4) at 400 °C (4.2 wt%). This outcome is unexpected, given that the carbonyl content and TAN value were reduced in the dewatered sample (Fig. 2), which would typically be associated with reduced coke formation. Bu et al. [77] suggested that methoxy-phenols are key coke precursors. As shown in Fig. 4, the dewatered pyrolysis oil contained a higher concentration of phenolic compounds, which may explain the increased formation of solid residues (char) during HDO. Another possible explanation is that higher solid product formation may be an inevitable by-product of achieving more extensive deoxygenation. Our GCxGC/MS results (Figs. 6 and 7) indicate that deoxygenation activity was greater with DPO. This will be discussed further in Section 3.3.1. If solid formation is indeed linked to this process, then increased char production could be expected. The removal of light volatile components and highly water-soluble species — preferentially extracted during dewatering — may leave behind molecules more prone to condense or polymerize under the reaction conditions, contributing to higher char yields. Interestingly, under identical reaction conditions, DPO1 produced a slightly higher total water yield (26 wt%) compared to PO4 (25.8 wt%). For DPO1, this included 3.2 wt% of initial water in the feed and 22.8 wt% generated during the HDO process (Fig. 5). In contrast, PO4 produced only 3.2 wt% of water during the reaction. The higher HDO activity of DPO should contribute to its apparent higher generation of water during its upgrading. Furthermore, elemental analysis of the solid products from DPO1 and PO4 revealed differences in composition. The solids from DPO1 contained 50.2% carbon, 43.3% oxygen, and 6.5% hydrogen, while the solids from PO4 contained 32.2% carbon and 63.3% oxygen. These results indicate that in both cases, a portion of the oxygen remained in the solid fraction.

3.3.1. GC-detectable compound distributions following HDO

Gas chromatography–mass spectrometry (GC–MS) is broadly implemented to identify chemical compounds in pyrolysis bio-oil, but it only detects a portion of the compounds present [53,78]. Accordingly, nuclear magnetic resonance (NMR) spectroscopy is often employed as one of the most comprehensive spectroscopic techniques for analyzing the full spectrum of bio-oil components [79]. In this study, GCxGC–MS/FID was used for qualitative analysis of the complex bio-oil samples [53,80], while two dimensional HSQC NMR served as a complementary technique to characterize both the pyrolysis bio-oil feedstocks and their corresponding upgraded oils, which will be discussed in Section 3.3.2.

The organic compounds in the aqueous phase were below detection limit of GC–MS, so the analysis focused on the upgraded oil, which consists of the organic phase rich in hexadecane. A classification based on chemical structure and functional groups — similar to that employed for the feedstock samples (described in Section 3.1) — was applied to the upgraded oils obtained from hydrodeoxygenation of the original and dewatered pyrolysis oils using sulfided $NiMo/Al_2O_3$ at 400 °C (PO4, and DPO1). This classification also included oxygen-free compounds (hydrocarbons). However, approximately 40% of the compounds in the upgraded oils (based on blob volume) had a very low match probability (<10%) in the NIST library and were therefore categorized as unidentified. Additionally, large oligomers present in bio-oils are not detectable by GCxGC and are excluded from this analysis. Table S3 lists all the compounds identified in the upgraded oils by GC–MS, along with their retention times. To account for potential cracking of hexadecane (used as the solvent) during the high temperature process [81], a control experiment was performed using only the solvent and catalyst under the same conditions as DPO1 and PO4. Fig. 6 presents the GC × GC chromatograms of the upgraded oils alongside the cracked fractions obtained from hexadecane. Consequently, the compound distribution in the upgraded oils was evaluated excluding the blobs from hexadecane and its cracking products, as shown in Fig. S4. The GC results provide a qualitative overview of the product distributions, highlighting both oxygenates and hydrocarbons, in the upgraded original and dewatered pyrolysis oils (Fig. 6a and b). In the upgraded oil samples, various oxygenates — including esters, ketones, and alcohols etc. — were detected along with hydrocarbons such as: cyclic hydrocarbons (e.g. cyclohexane, and cyclopentane, methyl-), aromatic hydrocarbons (e.g. propylbenzene, toluene, 1,2,3,4-tetrahydronaphthalene, o-xylene) and polyaromatic hydrocarbons (e.g. 2,4'-dimethyl-1,1'-biphenyl, 8,9-dehydro-9-vinyl-cycloisolongifolene, and 8-isopropyl-1,3-dimethylphenanthrene). In the case of the upgraded dewatered pyrolysis oil, trace amounts of phenols — such as 3-propylphenol, and 2,4-dimethylphenol, were also detected.

As shown in Fig. 7, the upgraded DPO contains a higher percentage of hydrocarbons (41.4%) and a lower percentage of oxygenates (19.3%) compared to the upgraded original pyrolysis oil (33.0% hydrocarbons and 26.3% oxygenates), indicating a greater degree of deoxygenation. During the upgrading/HDO process, various reactions take place [82], with oxygen being removed as carbon oxides by decarboxylation and decarbonylation (collectively DCO_x) into the gas phase. Water is produced through hydrodeoxygenation, dehydration, esterification, and aldol condensation reactions [22].

For the dewatered pyrolysis oil, both increased deoxygenation and greater solid formation were observed (Fig. 5). The higher solid yield may be due to enhanced overall reaction rates and activity. In addition, differences in chemical composition were noted in the upgraded oils. To better illustrate these differences, the hydrocarbons detected by GC/MS were classified into aromatic, cycloaliphatic (naphthenic), and acyclic aliphatic hydrocarbons (including linear and branched alkanes, alkenes, and alkynes) (Fig. 7). Based on each group's share of the total hydrocarbon peak volume, the upgraded dewatered oil exhibited a higher proportion of naphthenic and acyclic aliphatic hydrocarbons, whereas aromatic hydrocarbons were present in smaller amounts. This difference points to enhanced hydrogenation activity during HDO of the dewatered oil. The change in the proportion of acyclic aliphatics is relatively small, whereas the most pronounced differences occur in the naphthenic and aromatic fractions.

Regarding oxygenated compounds, the GC/MS detectable compounds in the upgraded DPO were primarily composed of alcohols, whereas the upgraded PO was dominated by esters and ethers, but also with a large amount of alcohols.

3.3.2. Solid product characteristics following HDO

To assess the impact of dewatering on coking, the combined mixture of spent catalysts and solid products from the HDO experiments with both PO and DPO were analyzed using elemental analysis. The results show distinct differences in the elemental composition between the

Table 3
Properties of the catalyst used in this study.

Catalyst	Active metal, (wt%)		Surface area (m^2g^{-1})	Pore volume (cm^3g^{-1})
$NiMo/Al_2O_3$	Ni 3.75	Mo 12.30	115.5 ± 7.9	0.28 ± 0.02

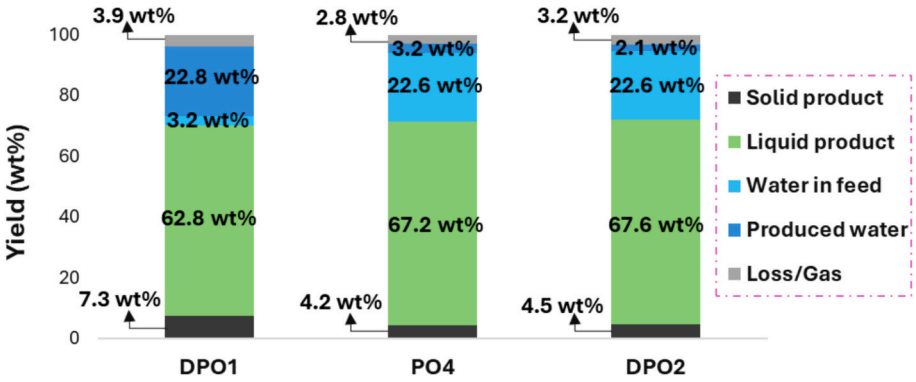

Fig. 5. Mass balance for the catalytic hydrotreatment of pyrolysis oil (PO4), dewatered oil (DPO1) and rehydrated DPO (DPO2) using 0.4 g $NiMoS/Al_2O_3$ catalyst, 2 g feedstock over 4 h reaction period (T: 400 °C, P: 30 bar H_2 at room temperature).

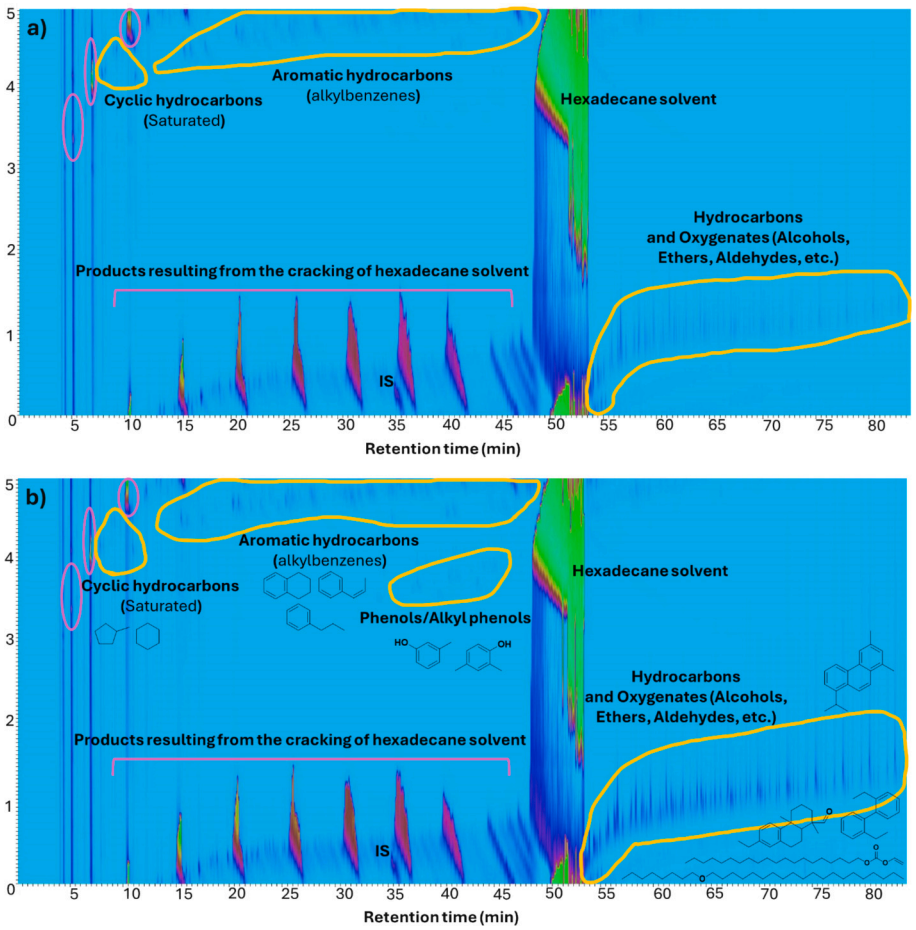

Fig. 6. Chromatograms (GC × GC–MS/FID) of the detectable liquid products obtained from: a) upgrading of pyrolysis oil, and b) upgrading of dewatered oil. Reaction conditions: 400 °C, initial H_2 pressure 73 bar, 0.4 g of NiMoS catalyst, 2 g of each oil feedstock sample.

solids between the two experiments (Table S4). The solids from the DPO1 experiment contained more carbon and less hydrogen than that from PO4, resulting in lower H/C and O/C molar ratios (Table S4). These characteristics suggest a more condensed, more dehydrogenated, and more coke-like deposit (often referred to as hard coke) [83,84], consistent with the higher solid yield observed during HDO of DPO. In contrast, the solid from PO4 showed higher H/C and O/C ratios, typical of more oxygen-rich, lightly polymerized deposits (light coke).

In summary, the dewatering process was effective in enhancing the upgrading performance by increasing the overall reaction rates and deoxygenation. This was evident from the higher concentration of deoxygenated products, and by the increased water generation during upgrading (Fig. 5). The additional water was visually confirmed by the presence of water droplets in a separate phase on the reactor vessel wall. However, this improvement came with a small increase in solid formation with more hard coke formed.

3.3.3. Insights from NMR analysis of pyrolysis-based feedstocks and their upgraded oils

To understand the changes in chemical composition resulting from the dewatering of pyrolysis oil — including both GC-detectable compounds and higher molecular weight fractions — 2D-HSQC NMR and ^1H

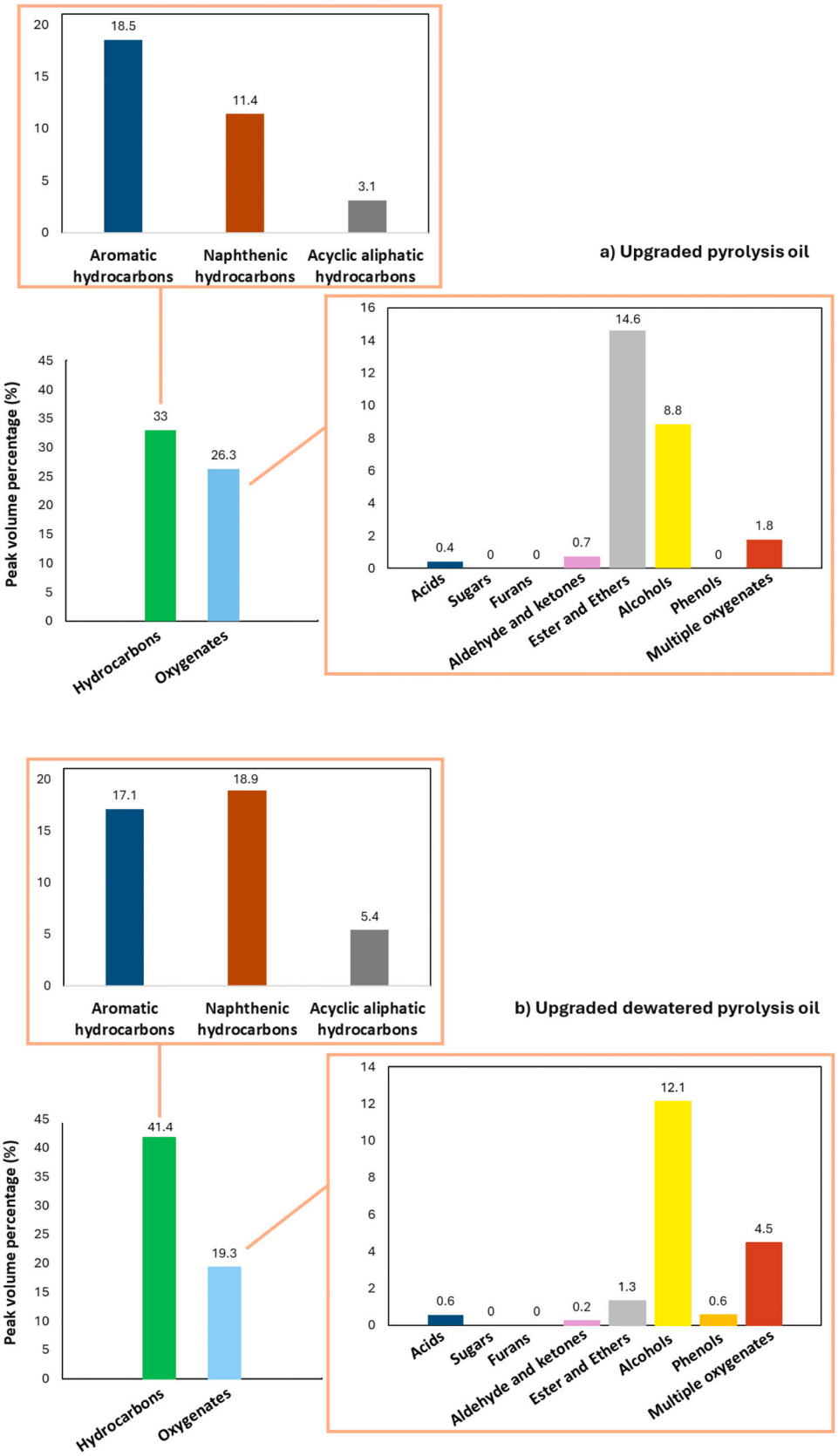

Fig. 7. GC-MS analysis comparing product distributions of hydrocarbon and oxygenate compounds from the upgrading of a) pyrolysis oil, and b) dewatered pyrolysis oil.

NMR analyses were performed on the original (PO) and dewatered (DPO) pyrolysis oils. For each feedstock oil sample (PO and DPO), the oil was first dissolved in methanol, after which $CDCl_3$ was added as the deuterated solvent. As a result, the dominant ^1H NMR peaks at 2.8–2.9 ppm (CH_3) and 4.4–4.5 ppm (OH) from methanol, together with the strong methanol line observed in the 2D-NMR spectra, were excluded from interpretation. Additionally, NMR was used to investigate the molecular transformations occurring during the hydrotreatment process by analyzing the upgraded oils derived from DPO1 and PO4. Two intense ^1H NMR resonances at about 0.85 ppm (terminal CH_3) and 1.25–1.35 ppm (–CH_2– groups), as well as the corresponding strong feature in the 2D-NMR spectra, attributable to hexadecane, were likewise omitted from the analysis. These results are presented in Figs. 8 and 8, and in the Supplementary information (Figs. S5 and S6).

The 2D NMR spectra of the feedstock oils, shown in Fig. 8, can be qualitatively interpreted by dividing the spectrum into three key regions based on characteristic chemical shifts, as reported in the literature [80,85,86]:

- Aliphatic region ($\delta C/\delta_H$ 10–48 / 0.5–2.7 ppm): This region primarily contains signals from saturated C—H bonds, typically arising from aliphatic chains and side groups.
- Oxygenated aliphatic region ($\delta C/\delta_H$ 52–105 / 2.8–5.7 ppm): Signals in this region correspond to protons adjacent to ether, hydroxyl, and carbonyl groups, common in compounds such as ketones and sugar derivatives. Methoxy substituents from aromatic structures like guaiacols also appear distinctly within this region.
- Aromatic and olefinic region ($\delta C/\delta_H$ 105–155 / 4.9–9.2 ppm): This region is characterized by signals from aromatic rings and unsaturated C═C bonds.

Together, these spectral features collectively reflect the complex chemical nature of pyrolysis oil components.

Upon comparing the NMR spectra of the feedstock oils on a

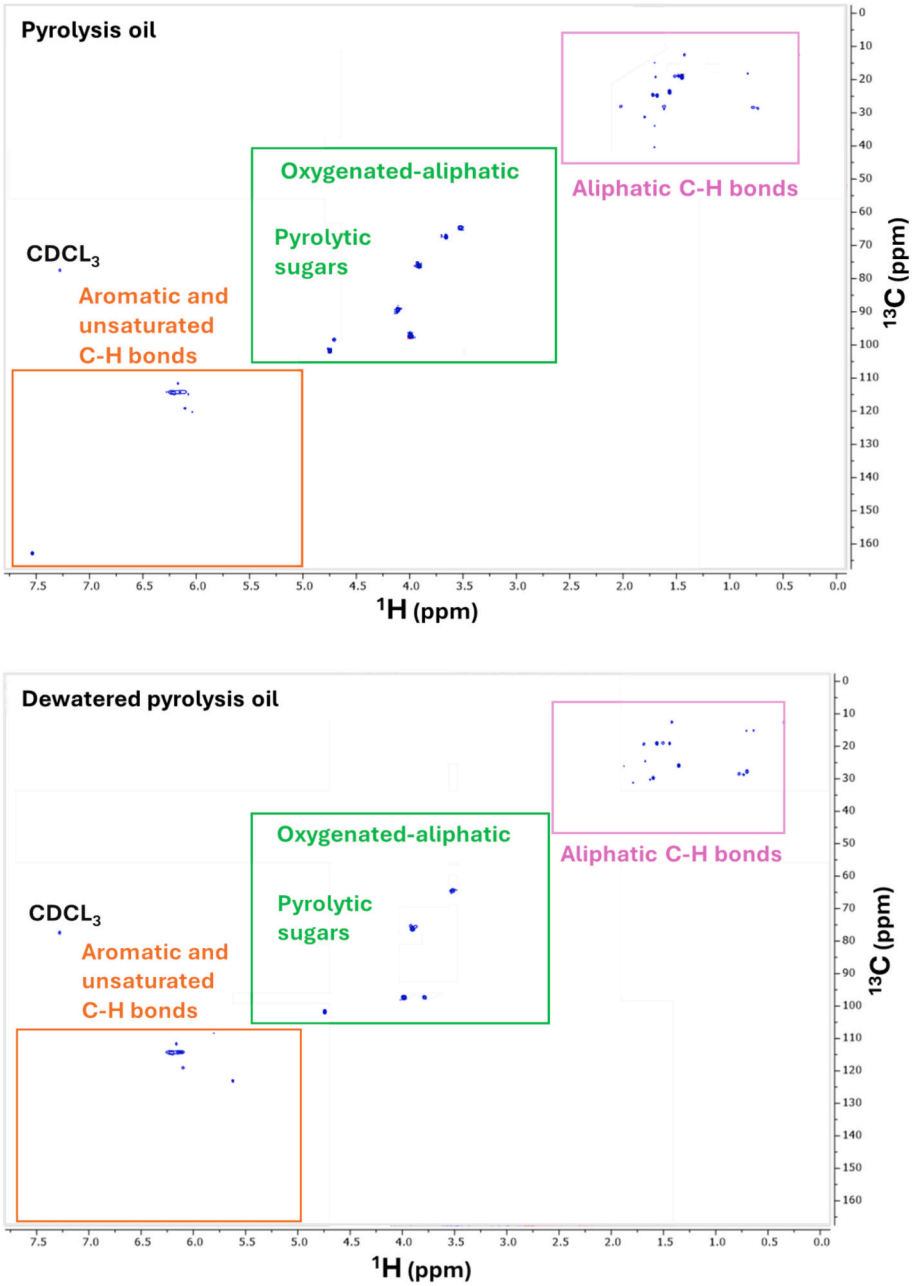

Fig. 8. Representative 2D-HSQC-NMR analyses of pyrolysis oil (top) and dewatered pyrolysis oil (bottom). $CDCl_3$ is the solvent.

consistent scale (Figs. 8 and S5), distinct changes were observed across all three spectral regions following the dewatering process. In the aliphatic region, DPO showed a marked decrease in signal intensity, particularly in the 2–1 ppm range of the ^{1}H NMR (Fig. S5). This range corresponds to methyl and methylene adjacent to aromatic rings and carbonyl functionalities, indicating a partial loss or transformation of these structures during dewatering. The oxygenated aliphatic region (2.8–5.7 ppm; see zoomed views in Figs. S5a and S5b, excluding methanol peaks) also exhibited a decline in signal intensity, which is associated with C—H bonds adjacent to ether, hydroxyl, and carbonyl groups—functionalities commonly found in sugars and other oxygenated species. GC analysis indicated a small reduction in sugar content (Fig. 4), consistent with the NMR observations, but also revealed an increase in GC-detectable multiple oxygenates. However, the overall decrease in NMR signal intensity in this region (Fig. S5) suggests that heavier oligomeric oxygenates — NMR-visible but not GC-detectable — were likely removed during dewatering. This interpretation is supported by GPC results (Table 1), which show a lower average molecular weight for DPO. Further evidence comes from elemental analysis, which revealed a decrease in the O/C ratio in DPO compared to PO (0.75 vs. 0.33, Table 1), indicating a general loss of oxygen-rich species. Additionally, carbonyl group quantification revealed a reduction in carbonyl content in DPO, directly supporting the weakened signals observed in the oxygenated aliphatic region of the NMR spectra. In the aromatic/olefinic region, at least one prominent peak disappeared after dewatering (Fig. S5), pointing to the removal or degradation of certain lignin-derived or unsaturated aromatic species. Collectively, these spectral changes indicate that the dewatering process not only removed water but also extracted fractions of both light and heavy oxygenates along with aromatic compounds.

The 2D-HSQC NMR and ^{1}H NMR spectra of the upgraded oils derived from PO and DPO reveal notable differences, particularly the absence of pyrolytic sugar signals and a more pronounced region corresponding to aromatic and unsaturated C—H bonds (δ_H 6.5–8.0 ppm / δ_C 110–150 ppm) in the upgraded DPO oil (Figs. 9 and S6). This sample exhibits more intense and numerous cross-peaks in this region (orange box in Fig. 9), suggesting the formation or preservation of substituted aromatic structures during hydrotreatment. These observations correspond well with the GC × GC-MS analysis, which showed a lower concentration of oxygenates — especially sugars — and a higher abundance of GC-detectable hydrocarbons in the upgraded DPO sample (Fig. 7). This interpretation is supported by the experimental data: although the PO feedstock had a higher initial water content (22.8 wt%), it produced less water (3.2 wt%) and lower char yields during hydrotreatment. In contrast, the DPO feedstock, with only 3.2 wt% initial water, generated 22.6 wt% water and exhibited higher char formation. These results indicate that the DPO-derived oil underwent a more extensive deoxygenation process, particularly involving phenolic and alcohol functionalities, leading to water release as a byproduct of hydrodeoxygenation and condensation reactions.

Although both upgraded oils showed broadly similar patterns in the oxygenated aliphatic region (Fig. S6), a direct comparison of the aliphatic region ($\delta C/\delta_H$ 10–48 ppm / 0.5–2.7 ppm) was limited due to the presence of hexadecane (C16) solvent in upgraded oils during NMR acquisition (Figs. 9 and S6). The strong aliphatic signals from C16 overlapped with sample peaks, obscuring much of this region (Figs. 9 and S6), and hindering a clear assessment of potential differences between the two oils. Nevertheless, the most pronounced changes were observed in the aromatic region. The upgraded DPO-derived oil exhibited higher signal intensity in the δ_H 5.0-6 ppm and 7.0-7.5 ppm ranges, with corresponding carbon shifts around δ_C 110–145 ppm (Figs. 9 and S6), indicating the formation or retention of substituted aromatic structures. Taken together, the NMR data, GC × GC-MS results, and water formation trends suggest that the DPO sample — richer in GC detectable phenolic compounds and multiple oxygenates — underwent more extensive hydrodeoxygenation. This led to increased water formation, enhanced aromatic content, but also a greater degree of condensation reactions, ultimately contributing to higher char production.

3.3.4. Proposed upgrading pathways and product distribution

To illustrate the key chemical transformations occurring during dewatering and subsequent HDO, Fig. 10 presents a schematic summary of the compositions of the pyrolysis oil, the dewatered oil, and the resulting upgraded oils. The scheme highlights representative major compounds from the different chemical classes observed in the GCxGC/MS measurements (as shown in Fig. 7), along with the associated solid formation. The top section of Fig. 10 shows the original pyrolysis oil, followed by the dewatering step and the composition of the resulting dewatered pyrolysis oil (DPO). GC analysis indicated that although the DPO remains rich in sugar-derived compounds, the dewatering process selectively removes certain species — most notably acetic acid — leading to a higher relative concentration of phenolics and multi-oxygenated compounds compared to the original pyrolysis oil.

The subsequent section in Fig. 10 presents the upgraded oils obtained from both PO and DPO. Many of the same or similar oxygenates and hydrocarbons are detected in both upgraded products, but their abundances differ significantly. In the upgraded DPO, naphthenic hydrocarbons are the most abundant class, followed by aromatic hydrocarbons, reflecting that cyclization and hydrogenation are more strongly promoted during HDO of the dewatered feed. Additionally, the cyclic compounds containing two to three rings (detected by GC × GC/MS) may partly originate from the breakdown of heavy oligomers present in the feed during the upgrading process. In contrast, the upgraded PO is dominated by aromatic hydrocarbons, with esters as the second most abundant group. The differences in oxygenated compounds between the two upgraded oils arise from the interplay between initial feed compositions and the deoxygenation pathways active during upgrading. For example, the removal of acids during dewatering limits ester formation in the upgraded DPO, whereas the upgraded PO contains higher levels of alcohols that can participate in esterification. Notably, methoxy-phenols are detected exclusively in the upgraded DPO, which may contribute to polymerization reactions and the observed increase in solid formation.

Overall, the chemical transformations during upgrading involve key deoxygenation reactions alongside enhanced cyclization and/or oligomer-breaking pathways. This is supported by the presence of several cyclic and polycyclic hydrocarbons in the upgraded oils, particularly in the upgraded DPO, indicating that hydrogenation and cyclization, together with the breakdown of oligomeric species, play major roles in restructuring hydrocarbons during HDO.

3.4. Understanding how dewatering influences hydrotreatment oil products

To determine whether the lower deoxygenation observed with PO is primarily due to its higher initial water content — potentially inhibiting or poisoning catalytic active sites — or to its higher concentration of acids and carbonyl compounds, an extra hydrotreatment experiment was performed using DPO. A controlled amount of water was added to the DPO to match the water content of PO (22.6 wt%), and the mixture underwent hydrotreatment under identical reaction conditions as those for PO and DPO (Table 1, DPO2). This approach allowed isolation of the effect of water content and clearer assessment of the impact of organic compositional changes resulting from the dewatering process. As shown in Fig. 5, reintroducing water to DPO suppressed catalytic activity, causing DPO to behave similarly to PO despite their differences in organic composition (DPO2 vs. PO4). This indicates that restoring water content reinstates water-related catalyst inhibition, leading to reduced catalytic activity and comparable amounts of water and solids produced during hydrotreatment of PO and rehydrated DPO. Water is known to inhibit or poison catalytic sites — particularly through oxidation of the

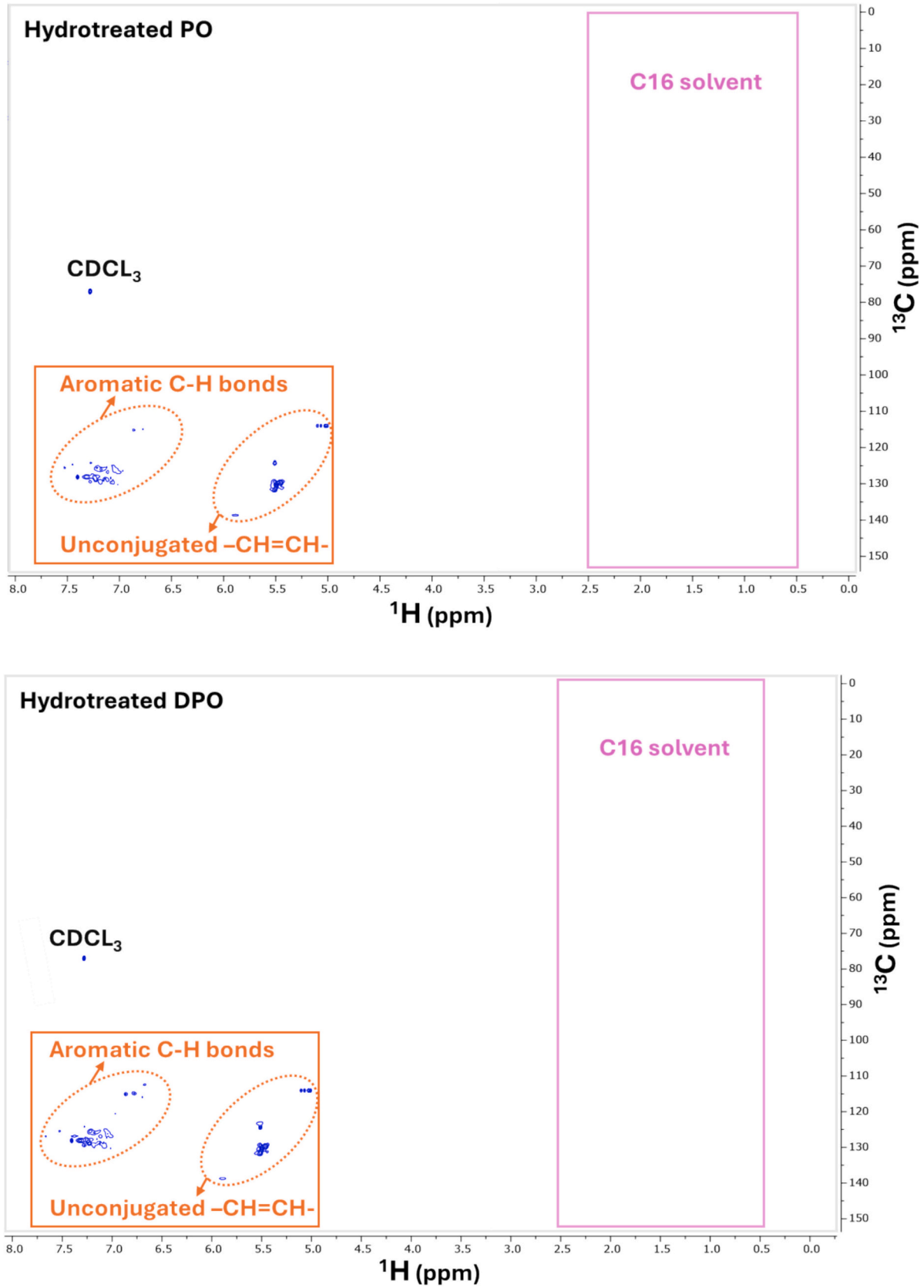

Fig. 9. Representative 2D-HSQC-NMR analyses of upgraded pyrolysis oil (top) and upgraded dewatered pyrolysis oil (bottom). $CDCl_3$ is the solvent.

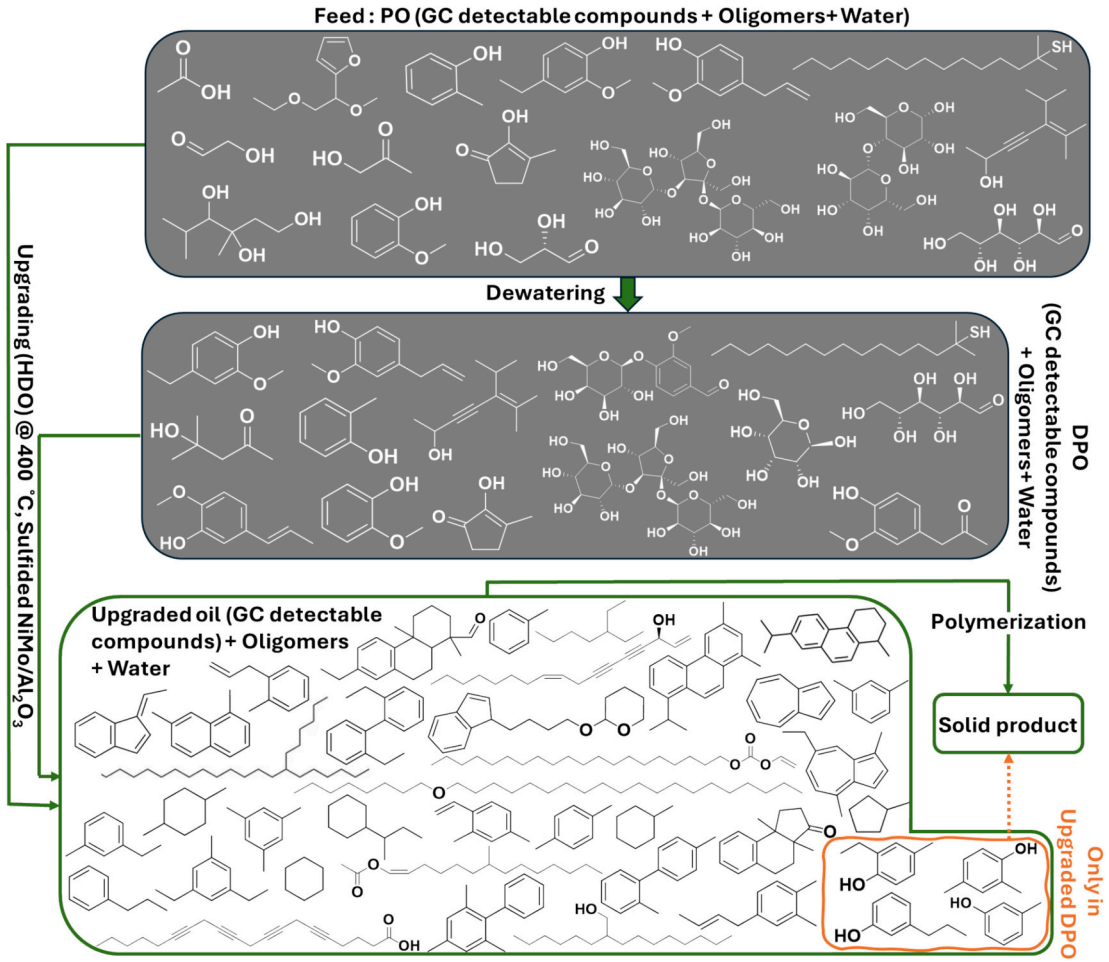

Fig. 10. Schematic representation of the transformation of pyrolysis oil (PO) to dewatered pyrolysis oil (PO), followed by upgrading (catalytic HDO) of both oils.

active metal sulfide phase — or via competitive adsorption or site blocking, which diminishes catalyst efficiency and lowers deoxygenation rates [87–89]. Therefore, although the oxygenated compounds removed during dewatering remain absent in DPO2, the dominant influence of water-induced catalyst inhibition governs the observed reaction behavior. Notably, this experiment was repeated twice to ensure reproducibility (see Table S2), yielding consistent results with solid yields of approximately 4.0 and 4.5 wt% and similar water production, confirming the reliability of the observed trends. Overall, these findings demonstrate that restoring water content reinstates water-related catalyst inhibition, reducing catalyst activity and resulting in similar levels of water and solid formation in both PO and rehydrated DPO samples.

4. Conclusions

The impact of water removal on pyrolysis oil characteristics — including acidity, heating value, stability, chemical composition, and its influence on the efficiency of a subsequent hydrotreatment upgrading process was systematically investigated. Dewatering of a pyrolysis oil via azeotropic distillation with mesityl oxide significantly improved the oil's properties. This process reduced acidity, increased the higher heating value (HHV), and altered the chemical composition by removing both volatile and heavy oxygenated compounds. GCxGC-MS and NMR analyses confirmed the removal of species with good solubility in water and/or mesityl oxide, such as sugars and acidic compounds, along with a decrease in carbonyl content, resulting in the concentration of more complex oxygenates. Accelerated aging demonstrated that the dewatered oil exhibited enhanced stability, characterized by reduced conversion of light compounds, minimal molecular weight increase, and slightly lower water formation compared to untreated pyrolysis oil. These improvements could be attributed to the reduced acidity and carbonyl content, which restrict aging reactions. Hydrotreatment of the dewatered oil using a $NiMoS/Al_2O_3$ catalyst at 400 °C, resulted in a higher degree of deoxygenation according to GCxGC-MS and NMR data. However, this also resulted in increased char formation. To isolate the effect of water on catalyst performance during HDO, water was reintroduced into the dewatered pyrolysis oil prior to upgrading. This rehydrated sample underwent hydrotreatment under identical conditions. The addition of water suppressed catalyst activity, indicating that water-induced inhibition — likely via competitive adsorption or site blocking — plays a dominant role in modulating catalyst performance, rather than changes in the organic composition. As a result, the reaction behavior and product distributions of the rehydrated sample closely resembled those of untreated pyrolysis oil. Overall, these findings underscore the critical role of water removal prior to hydrotreatment upgrading for enhancing catalyst efficiency and improving overall process performance.

CRediT authorship contribution statement

Elham Nejadmoghadam: Writing – original draft, Methodology, Investigation, Formal analysis, Data curation, Conceptualization. **Olov Öhrman:** Writing – review & editing, Supervision, Methodology, Funding acquisition, Conceptualization. **Derek Creaser:** Writing – review & editing, Supervision, Methodology, Conceptualization. **Louise Olsson:** Writing – review & editing, Supervision, Methodology, Funding

acquisition, Conceptualization.

Declaration of competing interest

The authors declare the following financial interests/personal relationships which may be considered as potential competing interests: Olov Öhrman reports financial support was provided by VAROPreem. Olov Öhrman reports a relationship with VAROPreem that includes: employment. Louise Olsson reports a relationship with VAROPreem that includes: funding grants. Elham Nejadmoghadam reports a relationship with VAROPreem that includes: funding grants. Louise Olsson is one of the Editors of Chemical Engineering Journal. If there are other authors, they declare that they have no known competing financial interests or personal relationships that could have appeared to influence the work reported in this paper.

Acknowledgements

This work has been performed at the Competence Centre for Catalysis (KCK) and the Chemical Engineering division at the Chalmers University of Technology in collaboration with VAROPreem. The funding from Formas (FR-2021/0005), Swedish Energy Agency (P2023-01506) and VAROPreem is gratefully acknowledged.

Appendix A. Supplementary data

Supplementary data to this article can be found online at https://doi.org/10.1016/j.cej.2026.174193.

Data availability

Data will be made available on request.

References

[1] M. Antar, D. Lyu, M. Nazari, A. Shah, X. Zhou, D.L. Smith, Biomass for a sustainable bioeconomy: an overview of world biomass production and utilization, Renew. Sust. Energ. Rev. 139 (2021) 110691.
[2] H. El Bari, C.K. Fanezoune, B. Dorneanu, H. Arellano-Garcia, T. Majozi, Y. Elhenawy, O. Bayssi, A. Hirt, J. Peixinho, A. Dhahak, Catalytic fast pyrolysis of lignocellulosic biomass: recent advances and comprehensive overview, J. Anal. Appl. Pyrolysis 106390 (2024).
[3] Z.-C. Wang, J. Duo, Y.-Q. Shan, L.-X. Yin, P.-G. Duan, Hydro-upgrading of bio-oils derived from pyrolysis of biomass with different H/Ceff ratios in tetralin over Pt/C and Ru/C, Int. J. Hydrog. Energy 48 (2023) 6916–6926.
[4] P. Lahijani, M. Mohammadi, A.R. Mohamed, F. Ismail, K.T. Lee, G. Amini, Upgrading biomass-derived pyrolysis bio-oil to bio-jet fuel through catalytic cracking and hydrodeoxygenation: a review of recent progress, Energy Convers. Manag. 268 (2022) 115956.
[5] A.I. Osman, M. Farghali, I. Ihara, A.M. Elgarahy, A. Ayyad, N. Mehta, K.H. Ng, E. M. Abd El-Monaem, A.S. Eltaweil, M. Hosny, Materials, fuels, upgrading, economy, and life cycle assessment of the pyrolysis of algal and lignocellulosic biomass: a review, Environ. Chem. Lett. 21 (2023) 1419–1476.
[6] E. Struhs, S. Hansen, A. Mirkouei, M.M. Ramirez-Corredores, K. Sharma, R. Spiers, J.H. Kalivas, Ultrasonic-assisted catalytic transfer hydrogenation for upgrading pyrolysis-oil, Ultrason. Sonochem. 73 (2021) 105502.
[7] Bioenergy from Boreal Forests: Swedish Approach to Sustainable Wood Use, 2019.
[8] T. Janosik, A.N. Nilsson, A.-C. Hällgren, M. Hedberg, C. Bernlind, H. Rådberg, L. Ahlsén, P. Arora, O.G.W. Öhrman, Derivatizing of fast pyrolysis bio-oil and Coprocessing in fixed bed Hydrotreater, Energy Fuel 36 (2022) 8274–8287, https://doi.org/10.1021/acs.energyfuels.2c01608.
[9] A.P. Pinheiro Pires, J. Arauzo, I. Fonts, M.E. Domine, A. Fernandez Arroyo, M. E. Garcia-Perez, J. Montoya, F. Chejne, P. Pfromm, M. Garcia-Perez, Challenges and opportunities for bio-oil refining: a review, Energy Fuel 33 (2019) 4683–4720.
[10] F.W. Brodin, J. Celaya Romeo, K. Toven, Dewatered pyrolysis oil as fuel component in marine fuel blends, in: In: 24th European Biomass Conference and Exhibition (EUBCE 2016), June 6-9, 2016, 2016, pp. 1122–1124. Amsterdam, Netherlands.
[11] M. Shahzeb Khan, M. Rafiq, V. Sookrah, M.J. Thomson, Effect of dewatering wood-derived fast pyrolysis oil on its fuel properties for power generation, Energy Fuel 33 (2019) 12403–12420.
[12] P. Roy, H. Jahromi, T. Rahman, J. Baltrusaitis, A. Torbert, S. Adhikari, Hydrotreatment of pyrolysis bio-oil with non-edible carinata oil and poultry fat for producing transportation fuels, Fuel Process. Technol. 245 (2023) 107753.
[13] F. Stankovikj, A.G. McDonald, G.L. Helms, M.V. Olarte, M. Garcia-Perez, Characterization of the water-soluble fraction of woody biomass pyrolysis oils, Energy Fuel 31 (2017) 1650–1664.
[14] H. Jahromi, S. Adhikari, P. Roy, E. Hassani, C. Pope, T.-S. Oh, Y. Karki, Production of green transportation fuels from Brassica carinata oil: a comparative study of noble and transition metal catalysts, Fuel Process. Technol. 215 (2021) 106737.
[15] M.Z. Stummann, M. Høj, J. Gabrielsen, L.R. Clausen, P.A. Jensen, A.D. Jensen, A perspective on catalytic hydropyrolysis of biomass, Renew. Sust. Energ. Rev. 143 (2021) 110960.
[16] M.L. Chacón-Patiño, C. Mase, J.F. Maillard, C. Barrère-Mangote, D.C. Dayton, C. Afonso, P. Giusti, R.P. Rodgers, Petroleomics approach to investigate the composition of upgrading products from pyrolysis bio-oils as determined by high-field FT-ICR MS, Energy Fuel 37 (2023) 16612–16628.
[17] S. Ahmadi, E. Reyhanitash, Z. Yuan, S. Rohani, C.C. Xu, Upgrading of fast pyrolysis oil via catalytic hydrodeoxygenation: effects of type of solvents, Renew. Energy 114 (2017) 376–382.
[18] G. Kim, J. Seo, J.-W. Choi, J. Jae, J.-M. Ha, D.J. Suh, K.-Y. Lee, J.-K. Jeon, J.-K. Kim, Two-step continuous upgrading of sawdust pyrolysis oil to deoxygenated hydrocarbons using hydrotreating and hydrodeoxygenating catalysts, Catal. Today 303 (2018) 130–135.
[19] F. Stankovikj, C.-C. Tran, S. Kaliaguine, M.V. Olarte, M. Garcia-Perez, Evolution of functional groups during pyrolysis oil upgrading, Energy Fuel 31 (2017) 8300–8316.
[20] F. Stankovikj, M. Garcia-Perez, TG-FTIR method for the characterization of bio-oils in chemical families, Energy Fuel 31 (2017) 1689–1701.
[21] E. Nejadmoghadam, A. Achour, P. Sirous-Rezaei, M.A. Salam, P. Arora, O. Öhrman, D. Creaser, L. Olsson, Stabilization of bio-oil from simulated pyrolysis oil using sulfided NiMo/Al2O3 catalyst, Fuel 353 (2023) 129094.
[22] Y. Han, M. Gholizadeh, C.C. Tran, S. Kaliaguine, C.Z. Li, M. Olarte, M. Garcia-Perez, Hydrotreatment of pyrolysis bio-oil: a review, Fuel Process. Technol. 195 (2019) 106140.
[23] X. Hu, Z. Zhang, M. Gholizadeh, S. Zhang, C.H. Lam, Z. Xiong, Y. Wang, Coke formation during thermal treatment of bio-oil, Energy Fuel 34 (2020) 7863–7914, https://doi.org/10.1021/acs.energyfuels.0c01323.
[24] A.L. Church, M.Z. Hu, S.-J. Lee, H. Wang, J. Liu, Selective adsorption removal of carbonyl molecular foulants from real fast pyrolysis bio-oils, Biomass Bioenergy 136 (2020) 105522.
[25] X. Junming, J. Jianchun, S. Yunjuan, L. Yanju, Bio-oil upgrading by means of ethyl ester production in reactive distillation to remove water and to improve storage and fuel characteristics, Biomass Bioenergy 32 (2008) 1056–1061.
[26] D.C. Elliott, S.-J. Lee, T.R. Hart, Stabilization of Fast Pyrolysis Oil: Post Processing Final Report, Pacific Northwest National Lab.(PNNL), in: Richland, WA (United States), 2012.
[27] S.B. Jones, C. Valkenburt, C.W. Walton, D.C. Elliott, J.E. Holladay, D.J. Stevens, C. Kinchin, S. Czernik, Production of gasoline and diesel from biomass via fast pyrolysis, hydrotreating and hydrocracking: a design case, Pacific Northwest National Lab.(PNNL-18284), Richland, WA (2009). United States.
[28] M.V. Olarte, A.H. Zacher, A.B. Padmaperuma, S.D. Burton, H.M. Job, T.L. Lemmon, M.S. Swita, L.J. Rotness, G.N. Neuenschwander, J.G. Frye, Stabilization of softwood-derived pyrolysis oils for continuous bio-oil hydroprocessing, Top. Catal. 59 (2016) 55–64.
[29] H. Wang, S.-J. Lee, M.V. Olarte, A.H. Zacher, Bio-oil stabilization by hydrogenation over reduced metal catalysts at low temperatures, ACS Sustain. Chem. Eng. 4 (2016) 5533.
[30] D. Han, W. Yin, A. Arslan, T. Liu, Y. Zheng, S. Xia, Stabilization of fast pyrolysis liquids from biomass by mild catalytic Hydrotreatment: model compound study, Catalysts 10 (2020) 402, https://doi.org/10.3390/catal10040402.
[31] W. Choi, H. Jo, J.-W. Choi, D.J. Suh, H. Lee, C. Kim, K.H. Kim, K.-Y. Lee, J.-M. Ha, Stabilization of acid-rich bio-oil by catalytic mild hydrotreating, Environ. Pollut. 272 (2021) 116180, https://doi.org/10.1016/j.envpol.2020.116180.
[32] E. Nejadmoghadam, A. Achour, O. Öhrman, M.A. Salam, D. Creaser, L. Olsson, Stabilization of fresh and aged simulated pyrolysis oil through mild hydrotreatment using noble metal catalysts, Energy Convers. Manag. 313 (2024) 118570.
[33] S. Xiu, A. Shahbazi, L. Wang, C.W. Wallace, Supercritical ethanol liquefaction of swine manure for bio-oils production, Am. Erican Journal Engineering Applied Science 3 (2010) 494–500.
[34] X. Han, H. Wang, Y. Zeng, J. Liu, Advancing the application of bio-oils by co-processing with petroleum intermediates: a review, Energy Convers. Manage.: X 10 (2021) 100069.
[35] A. Nomura, C.W. Jones, Amine-functionalized porous silicas as adsorbents for aldehyde abatement, ACS Appl. Mater. Interfaces 5 (2013) 5569–5577.
[36] T. Sundqvist, A. Oasmaa, A. Koskinen, Upgrading fast pyrolysis bio-oil quality by esterification and Azeotropic water removal, Energy Fuel 29 (2015) 2527.
[37] N. Bergvall, L. Sandström, F. Weiland, O.G.W. Öhrman, Corefining of fast pyrolysis bio-oil with vacuum residue and vacuum gas oil in a continuous slurry hydrocracking process, Energy Fuel 34 (2020) 8452.
[38] N. Bergvall, R. Molinder, A.-C. Johansson, L. Sandström, Continuous slurry hydrocracking of biobased fast pyrolysis oil, Energy Fuel 35 (2021) 2303.
[39] S. Van Dyk, M. Ebadian, J. Su, F. Larock, Y. Zhang, J. Monnier, H. Wang, D. M. Santosa, M.V. Olarte, G. Neuenschwander, Assessment of Likely Technology Maturation Pathways for Biojet Production from Forest Residues, Vancouver, 2019.
[40] B.-J. Lin, W.-H. Chen, W.M. Budzianowski, C.-T. Hsieh, P.-H. Lin, Emulsification analysis of bio-oil and diesel under various combinations of emulsifiers, Appl. Energy 178 (2016) 746–757.

[41] M.D.G. de Luna, L.A.D. Cruz, W.-H. Chen, B.-J. Lin, T.-H. Hsieh, Improving the stability of diesel emulsions with high pyrolysis bio-oil content by alcohol co-surfactants and high shear mixing strategies, Energy 141 (2017) 1416–1428.
[42] C.J. Mueller, The feasibility of using raw liquids from fast pyrolysis of woody biomass as fuels for compression-ignition engines: a literature review, SAE Int. J. Fuels Lubr. 6 (2013) 251–262.
[43] C.R. Vitasari, G.W. Meindersma, A.B. De Haan, Water extraction of pyrolysis oil: the first step for the recovery of renewable chemicals, Bioresour. Technol. 102 (2011) 7204–7210.
[44] F.H. Mahfud, I. Melian-Cabrera, R. Manurung, H.J. Heeres, Biomass to fuels: upgrading of flash pyrolysis oil by reactive distillation using a high boiling alcohol and acid catalysts, Process Saf. Environ. Prot. 85 (2007) 466–472.
[45] L. Moens, S.K. Black, M.D. Myers, S. Czernik, Study of the neutralization and stabilization of a mixed hardwood bio-oil, Energy Fuel 23 (2009) 2695–2699.
[46] T.M.H. Dabros, M.Z. Stummann, M. Høj, P.A. Jensen, J.-D. Grunwaldt, J. Gabrielsen, P.M. Mortensen, A.D. Jensen, Transportation fuels from biomass fast pyrolysis, catalytic hydrodeoxygenation, and catalytic fast hydropyrolysis, Prog. Energy Combust. Sci. 68 (2018) 268.
[47] J. Venuti Björkman, L. Lukovicsová, T. Belkheiri, S.L. Hruby, L.J. Pettersson, E. Kantarelis, Differences in apparent activity of Sulfided NiMo/γ-Al2O3 Hydrotreating catalysts elucidated by dynamic reactor modelling, Top. Catal. 68 (2025) 2494–2506.
[48] D.-P. Phan, T.K. Vo, J. Kim, E.Y. Lee, Spray pyrolysis synthesis of bimetallic NiMo/Al2O3–TiO2 catalyst for hydrodeoxygenation of guaiacol: effects of bimetallic composition and reduction temperature, J. Ind. Eng. Chem. 83 (2020) 351–358.
[49] C.R. Kumar, N. Anand, A. Kloekhorst, C. Cannilla, G. Bonura, F. Frusteri, K. Barta, H.J. Heeres, Solvent free depolymerization of Kraft lignin to alkyl-phenolics using supported NiMo and CoMo catalysts, Green Chem. 17 (2015) 4921–4930.
[50] A.-Ch. Hällgren, N.A. Nilsson, T. Janosik, Dewatering of Thermochemical Oil, WO2020245296A1, n.d.
[51] H. Ojagh, D. Creaser, S. Tamm, P. Arora, S. Nyström, E. Lind Grennfelt, L. Olsson, Effect of dimethyl disulfide on activity of NiMo based catalysts used in hydrodeoxygenation of oleic acid, Ind. Eng. Chem. Res. 56 (2017) 5547–5557.
[52] A.K. Varma, L.S. Thakur, R. Shankar, P. Mondal, Pyrolysis of wood sawdust: effects of process parameters on products yield and characterization of products, Waste Manag. 89 (2019) 224–235.
[53] M. Staš, M. Auersvald, L. Kejla, D. Vrtiška, J. Kroufek, D. Kubička, Quantitative analysis of pyrolysis bio-oils: a review, TrAC Trends Anal. Chem. 126 (2020) 115857.
[54] N. Charon, J. Ponthus, D. Espinat, F. Broust, G. Volle, J. Valette, D. Meier, Multi-technique characterization of fast pyrolysis oils, J. Anal. Appl. Pyrolysis 116 (2015) 18–26.
[55] E. Butler, G. Devlin, D. Meier, K. McDonnell, Fluidised bed pyrolysis of lignocellulosic biomasses and comparison of bio-oil and micropyrolyser pyrolysate by GC/MS-FID, J. Anal. Appl. Pyrolysis 103 (2013) 96–101.
[56] A. Oasmaa, D.C. Elliott, J. Korhonen, Acidity of biomass fast pyrolysis bio-oils, Energy Fuel 24 (2010) 6548–6554.
[57] F.A. Agblevor, A. Foster, Rapid method for the determination of total acid number (TAN) of biooils, in: AIChE 2010 Annual Meeting, 2010. Salt Lake City, USA.
[58] S. Black, J.R. Ferrell III, Determination of carbonyl groups in pyrolysis bio-oils using potentiometric titration: review and comparison of methods, Energy Fuel 30 (2016) 1071–1077.
[59] J.R. Ferrell III, M.V. Olarte, E.D. Christensen, A.B. Padmaperuma, R.M. Connatser, F. Stankovikj, D. Meier, V. Paasikallio, Standardization of chemical analytical techniques for pyrolysis bio-oil: history, challenges, and current status of methods, Biofuels, Bioproducts and Biorefining 10 (2016) 496–507.
[60] M.V. Olarte, S.D. Burton, M. Swita, A.B. Padmaperuma, J. Ferrell, H. Ben, Determination of Hydroxyl Groups in BIOREFIN, National Renewable Energy Lab. (NREL), in: Golden, 2016. CO (United States).
[61] X. Meng, C. Crestini, H. Ben, N. Hao, Y. Pu, A.J. Ragauskas, D.S. Argyropoulos, Determination of hydroxyl groups in biorefinery resources via quantitative 31P NMR spectroscopy, Nat. Protoc. 14 (2019) 2627–2647.
[62] H. Jiang, P. Lu, Z. Xue, D. Zhao, C. Bu, H. Ge, T. Song, Prediction and evaluation on fuel properties and pyrolysis characteristics of combustible industrial solid wastes, J. Energy Inst. 105 (2022) 232–241.
[63] R.J. French, J. Stunkel, R.M. Baldwin, Mild Hydrotreating of bio-oil: effect of reaction severity and fate of oxygenated species, Energy Fuel 25 (2011) 3266.
[64] G.O. Zasypalov, V.A. Klimovsky, E.S. Abramov, E.E. Brindukova, V.D. Stytsenko, A. P. Glotov, Hydrotreating of lignocellulosic bio-oil (a review), Pet. Chem. 63 (2023) 1143–1169.
[65] S. Jamilatun, B. Budhijanto, R. Rochmadi, A. Yuliestyan, H. Hadiyanto, A. Budiman, Comparative analysis between pyrolysis products of Spirulina platensis biomass and its residues, International Journal of Renewable Energy Development 8 (2019) 133.
[66] B. Scholze, C. Hanser, D. Meier, Characterization of the water-insoluble fraction from fast pyrolysis liquids (pyrolytic lignin): part II. GPC, carbonyl goups, and 13C-NMR, J. Anal. Appl. Pyrolysis 58 (2001) 387–400.
[67] A. Alvarez-Majmutov, S. Badoga, J. Chen, J. Monnier, Y. Zhang, Co-processing of deoxygenated pyrolysis bio-oil with vacuum gas oil through hydrocracking, Energy Fuel 35 (2021) 9983–9993.
[68] L.K.E. Park, J. Liu, S. Yiacoumi, A.P. Borole, C. Tsouris, Contribution of acidic components to the total acid number (TAN) of bio-oil, Fuel 200 (2017) 171–181.
[69] S. Martin, C. Josef, K. David, B. Josef, P. Milan, Petroleomic characterization of pyrolysis bio-oils: a review, Energy Fuel 31 (2017) 10283–10299.
[70] A. Oasmaa, I. Fonts, M.R. Pelaez-Samaniego, M.E. Garcia-Perez, M. Garcia-Perez, Pyrolysis oil multiphase behavior and phase stability: a review, Energy Fuel 30 (2016) 6179–6200.
[71] A. Oasmaa, E. Kuoppala, Fast pyrolysis of forestry residue. 3. Storage stability of liquid fuel, Energy Fuel 17 (2003) 1075–1084.
[72] J. Cai, M.M. Rahman, S. Zhang, M. Sarker, X. Zhang, Y. Zhang, X. Yu, E.H. Fini, Review on aging of bio-oil from biomass pyrolysis and strategy to slowing aging, Energy Fuel 35 (2021) 11665–11692.
[73] R. Wang, H. Ben, Accelerated aging process of bio-oil model compounds: a mechanism study, Front. Energy Res. 8 (2020) 79.
[74] J.P. Diebold, A Review of the Chemical and Physical Mechanisms of the Storage Stability of Fast Pyrolysis Bio-Oils, 1999.
[75] H. Sui, J. Shao, F.A. Agblevor, Y. Zhang, X. Wang, H. Yang, H. Chen, Fractional condensation and aging of pyrolysis oil from cotton stalk, Biomass Bioenergy 174 (2023) 106837.
[76] J. Meng, A. Moore, D.C. Tilotta, S.S. Kelley, S. Adhikari, S. Park, Thermal and storage stability of bio-oil from pyrolysis of torrefied wood, Energy Fuel 29 (2015) 5117–5126.
[77] Q. Bu, H. Lei, A.H. Zacher, L. Wang, S. Ren, J. Liang, Y. Wei, Y. Liu, J. Tang, Q. Zhang, A review of catalytic hydrodeoxygenation of lignin-derived phenols from biomass pyrolysis, Bioresour. Technol. 124 (2012) 470–477.
[78] K. Lu, N. Hao, X. Meng, Z. Luo, G.A. Tuskan, A.J. Ragauskas, Investigating the correlation of biomass recalcitrance with pyrolysis oil using poplar as the feedstock, Bioresour. Technol. 289 (2019) 121589.
[79] N. Hao, H. Ben, C.G. Yoo, S. Adhikari, A.J. Ragauskas, Review of NMR characterization of pyrolysis oils, Energy Fuel 30 (2016) 6863–6880.
[80] N. Priharto, F. Ronsse, W. Prins, I. Hita, P.J. Deuss, H.J. Heeres, Hydrotreatment of pyrolysis liquids derived from second-generation bioethanol production residues over NiMo and CoMo catalysts, Biomass Bioenergy 126 (2019) 84–93.
[81] Y.W. Cheah, R. Intakul, M.A. Salam, J. Sebastian, P.H. Ho, P. Arora, O. Öhrman, D. Creaser, L. Olsson, Slurry co-hydroprocessing of Kraft lignin and pyrolysis oil over unsupported NiMoS catalyst: a strategy for char suppression, Chem. Eng. J. 475 (2023) 146056.
[82] M. Benés, R. Bilbao, J.M. Santos, J. Alves Melo, A. Wisniewski Jr., I. Fonts, Hydrodeoxygenation of lignocellulosic fast pyrolysis bio-oil: characterization of the products and effect of the catalyst loading ratio, Energy Fuel 33 (2019) 4272–4286.
[83] M. Zhang, J. Huang, F. Meng, C. Zhang, Z. Zhang, Coke-induced deactivation in zeolite catalysts: mechanisms, anti-coking modifications, and regeneration approaches, Dalton Trans. 54 (2025) 17383–17399.
[84] I. Hita, T. Cordero-Lanzac, G. Bonura, F. Frusteri, J. Bilbao, P. Castaño, Dynamics of carbon formation during the catalytic hydrodeoxygenation of raw bio-oil, sustain, Energy Fuel 4 (2020) 5503–5512.
[85] D. Castello, S. He, M.P. Ruiz, R.J.M. Westerhof, H.J. Heeres, K. Seshan, S.R. A. Kersten, Is it possible to increase the oil yield of catalytic pyrolysis of biomass? A study using commercially-available acid and basic catalysts in ex-situ and in-situ modus, J. Anal. Appl. Pyrolysis 137 (2019) 77–85.
[86] T.A. Jambeiro, M.F.S. Silva, L.G.G. Pereira, D. da Silva Vasconcelos, G. Batalha Silva, M.B. Figueirêdo, S.B. Lima, C.A.M. Pires, Fast pyrolysis of sisal residue in a pilot fluidized bed reactor, Energy Fuel 32 (2018) 9478–9492.
[87] H. Wang, G. Li, K. Rogers, H. Lin, Y. Zheng, S. Ng, Hydrotreating of waste cooking oil over supported CoMoS catalyst–catalyst deactivation mechanism study, molecular, Catalysis 443 (2017) 228–240.
[88] M. Badawi, J.-F. Paul, S. Cristol, E. Payen, Y. Romero, F. Richard, S. Brunet, D. Lambert, X. Portier, A. Popov, Effect of water on the stability of Mo and CoMo hydrodeoxygenation catalysts: a combined experimental and DFT study, J. Catal. 282 (2011) 155–164.
[89] P.M. Mortensen, D. Gardini, C.D. Damsgaard, J.-D. Grunwaldt, P.A. Jensen, J. B. Wagner, A.D. Jensen, Deactivation of Ni-MoS2 by bio-oil impurities during hydrodeoxygenation of phenol and octanol, Appl. Catal. A Gen. 523 (2016) 159–170.